Inorg. Chem. **2007**, *46*, 11277–11290

Substituent Effects in Formally Quintuple-Bonded ArCrCrAr Compounds (Ar = Terphenyl) and Related Species

Robert Wolf,[†] Chengbao Ni,[†] Tailuan Nguyen,[†] Marcin Brynda,[†] Gary J. Long,[‡] Andrew D. Sutton,[†] Roland C. Fischer,[†] J. C. Fettinger,[†] Matthew Hellman,[§] Lihung Pu,[§] and Philip P. Power*,[†]

Departments of Chemistry, One Shields Avenue, University of California, Davis, Davis, California 95616, University of Missouri—Rolla, Rolla, Missouri 65409-0010, and California State University, Dominguez Hills, 1000 East Victoria Street, Carson, California 90747

Received October 25, 2007

The effects of different terphenyl ligand substituents on the quintuple Cr–Cr bonding in arylchromium(I) dimers stabilized by bulky terphenyl ligands (Ar) were investigated. A series of complexes, ArCrCrAr (**1**–**4**; Ar = C_6H_2-2,6-(C_6H_3-2,6-$^iPr_2$)$_2$-4-X, where X = H, $SiMe_3$, OMe, and F), was synthesized and structurally characterized. Their X-ray crystal structures display similar trans-bent C(ipso)CrCrC(ipso) cores with short Cr–Cr distances that range from 1.8077(7) to 1.8351(4) Å. There also weaker Cr–C interactions [2.294(1)–2.322(2) Å] involving an C(ipso) of one of the flanking aryl rings. The data show that the changes induced in the Cr–Cr bond length by the different substituents X in the para positions of the central aryl ring of the terphenyl ligand are probably a result of packing rather than electronic effects. This is in agreement with density functional theory (DFT) calculations, which predict that the model compounds (4-XC_6H_4)CrCr(C_6H_4-4-X) (X = H, $SiMe_3$, OMe, and F) have similar geometries in the gas phase. Magnetic measurements in the temperature range of 2–300 K revealed temperature-independent paramagnetism in **1**–**4**. UV–visible and NMR spectroscopic data indicated that the metal–metal-bonded solid-state structures of **1**–**4** are retained in solution. Reduction of (4-F_3CAr′)CrCl (4-F_3CAr′ = C_6H_2-2,6-(C_6H_3-2,6-$^iPr_2$)$_2$-4-CF_3) with KC_8 gave non-Cr–Cr-bonded fluorine-bridged dimer {(4-F_3CAr′)Cr(μ-F)(THF)}$_2$ (**5**) as a result of activation of the CF_3 moiety. The monomeric, two-coordinate complexes [(3,5-$^iPr_2$Ar*)Cr(L)] (**6**, L = THF; **7**, L = PMe_3; 3,5-$^iPr_2$Ar* = C_6H_1-2,6-(C_6H-2,4,6-$^iPr_3$)$_2$-3,5-$^iPr_2$) were obtained with use of the larger 3,5-Pr^i_2-Ar* ligand, which prevents Cr–Cr bond formation. Their structures contain almost linearly coordinated Cr^I atoms, with high-spin $3d^5$ configurations. The addition of toluene to a mixture of (3,5-$^iPr_2$Ar*)CrCl and KC_8 gave the unusual dinuclear benzyl complex [(3,5-$^iPr_2$Ar*)Cr(η^3:η^6-CH_2Ph)Cr(Ar*-1-H-3,5-$^iPr_2$)] (**8**), in which a C–H bond from a toluene methyl group was activated. The electronic structures of **5**–**8** have been analyzed with the aid of DFT calculations.

Introduction

Although the first compound with a metal−metal multiple bond, [$Cr_2(O_2CMe)_4(H_2O)_2$],[1] was synthesized in the mid-19th century, metal−metal multiple bonding was not authenticated until the landmark $[Re_2Cl_8]^{2-}$ dianion was structurally characterized in 1964.[2] Since then, the field has matured into a major research area in inorganic chemistry.[3] The development of increasingly complex ligands that stabilize new types of metal−metal multiple bonds is a constant feature of the literature.[4−8] For group 6 metals, "paddle-wheel" complexes of the type $[M_2L_4L'_{0-2}]$ (L =

* To whom correspondence should be addressed. E-mail: pppower@ucdavis.edu.
[†] University of California, Davis.
[‡] University of Missouri—Rolla.
[§] California State University.

(1) Peligot, E. *C. R. Hebd. Seances Acad. Sci.* **1844**, *19*, 609.
(2) Cotton, F. A.; Curtis, N. F.; Harris, C. B.; Johnson, B. F. G.; Lippard, S. J.; Mague, J. T.; Robinson, W. R.; Wood, J. S. *Science* **1964**, *145*, 1305.
(3) Cotton, F. A., Murillo, L. A., Walton, R. A., Eds. *Multiple Bonds between Metal Atoms*, 3rd ed.; Springer: Berlin, 2005.
(4) Chisholm, M. H.; Patmore, N. J. *Acc. Chem. Res.* **2007**, *40*, 19. Chisholm, M. H.; Patmore, N. J. *Chem. Rec.* **2005**, *5*, 308. Chisholm, M. H.; Macintosh, A. M. *Chem. Rev.* **2005**, *105*, 2949.
(5) Murillo, C. A.; Cotton, F. A. *Eur. J. Inorg. Chem.* **2006**, 2409.
(6) Cotton, F. A.; Gruhn, N. E.; Gu, J. D.; Huang, P.; Lichtenberger, D. L.; Murillo, C. A.; van Dorn, C. L.; Wilkinson, C. C. *Science* **2002**, *298*, 1971.
(7) Berry, J. F.; Cotton, F. A.; Tongbu, L.; Murillo, C. A.; Robert, B. K.; Wang, X. J. *J. Am. Chem. Soc.* **2004**, *126*, 7082. Kreisel, K. A.; Yap, G. P. A.; Theopold, K. H. *Chem. Commun.* **2007**, 1510.
(8) Tsai, J. C.; Lin, Y.-M.; Jen-Shiang, K. U.; Hwang, J.-K. *J. Am. Chem. Soc.* **2006**, *128*, 13980.

10.1021/ic702112e CCC: $37.00
Published on Web 11/29/2007

Chart 1

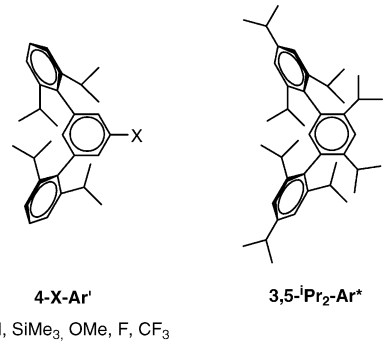

bridging bidentate ligand; L′ = axial ligand) have attracted considerable attention, particularly derivatives of chromium. Cotton has noted that "chromium is unique among the elements of the first transition series in its ability to form many compounds with multiple bonds in Cr_2^{4+} complexes."[3] The large variation in Cr−Cr distances, from ca. 1.83 to 2.60 Å, is particularly noteworthy, and the shortest metal−metal bond in a molecular species was found in the complex $[Cr_2(C_6H_3\text{-}2\text{-MeO-}5\text{-Me})_4]$ [Cr−Cr = 1.828(2) Å].[9]

Bulky terphenyl ligands,[10,11] such as C_6H_3-2,6-(C_6H_3-2,6-$^iPr_2)_2$[12] (abbreviated Ar′; Chart 1), have been widely used to stabilize new types of metal−metal bonds between the group 12−15 elements,[12−25] and, recently, we used the Ar′ ligand to stabilize Ar′CrCrAr′ (**1**), the first compound featuring a quintuple-bonding interaction.[23] The dimeric arylchromium(I) complex **1** was obtained by reduction of Ar′CrCl[26] with KC_8. It displayed a centrosymmetric, planar, trans-bent CCrCrC core structure with a very short Cr−Cr distance of 1.8351(4) Å. Theoretical calculations also indicated that **1** contained a Cr−Cr bond in which five orbitals from each metal center participitate in the bonding. The bond can, therefore, be *formally* described as a quintuple one, although the calculated *effective* bond order was 3.52.[23,27] Following this initial report, we were anxious to explore how changes in the steric and electronic properties of the terphenyl ligand might affect the metal−metal bonding. As a result, we developed ligands related to Ar′ (see Chart 1) with different electronic and steric properties. Herein, we report the synthesis and characterization of an ArCrCrAr series (**1**−**4**; Ar = C_6H_2-2,6-(C_6H_3-2,6-$^iPr_2)_2$-4-X, where X = H, $SiMe_3$, OMe, and F) as well as the dimeric chromium(II) fluoride $[(4\text{-}F_3CAr')Cr(\mu\text{-}F)(THF)]_2$ (**5**; THF = tetrahydrofuran), which is a decomposition product from the reduction of (4-F_3CAr′)CrCl with KC_8. We also investigated the steric influence of the very bulky ligand C_6H-2,6-(C_6H_2-2,4,6-^{i}-$Pr_3)_2$-3,5-$^iPr_2$[28] (abbreviated 3,5-$^iPr_2$Ar*) on Cr−Cr bonding. We recently communicated the isolation of the monomeric, two-coordinate chromium(I) complexes [(3,5-$^iPr_2$Ar*)Cr(L)] (**6**, L = THF; **7**, L = PMe_3) of this ligand.[29] We now present a full account of these studies as well as the preparation of the dinuclear complex [(3,5-$^iPr_2$Ar*)Cr(η^3:η^6-CH_2Ph)Cr(Ar*-1-H-3,5-$^iPr_2$)] (**8**), which was isolated by reduction of the precursor (3,5-$^iPr_2$Ar*)CrCl with KC_8 and subsequent extraction with toluene. Compounds **1**−**8** were characterized by X-ray crystallography, NMR and UV−visible spectroscopy, and magnetic measurements.

Experimental Section

General Considerations. All manipulations were carried out with the use of modified Schlenk techniques under an argon atmosphere or in a Vacuum Atmospheres HE-43 drybox. All solvents were dried by the method of Grubbs[30] and degassed three times (freeze−thaw) prior to use. The preparations of ArCrCl (Ar = C_6H_2-2,6-(C_6H_3-2,6-$^iPr_2)_2$-4-X, where X = H, $SiMe_3$, OMe, F, and CF_3) and (3,5-$^iPr_2$Ar*)CrCl are analogous to that described for $[Ar'CrCl]_2$,[26] and details are provided in the Supporting Information. The ArI and LiAr reagents (Ar = C_6H_3-2,6(C_6H_3-2,6-$^iPr_2)_2$-4-X, where *X* = H, OMe, and $SiMe_3$) were prepared as reported elsewhere.[31] ^{1}H NMR spectra were recorded on Varian 300 and 600 MHz instruments and referenced to the residual protiobenzene and toluene in the C_6D_6 solvent or the Me signal of the C_7D_8 solvent. The ^{19}F, ^{29}Si{^{1}H}, and ^{31}P{^{1}H} NMR spectra were recorded on a Varian 300 MHz NMR spectrometer and referenced against external standards (BF_3·OEt_2, $SiMe_4$, or H_3PO_4, respectively). The assignment of signals in the ^{1}H NMR spectra of **1** and **3** has been established with the aid of a COSY spectrum. C and H combustion data for **3** and **4** suggested that some loss of solvent had occurred, while data for **5** and **8** that were in good agreement with the calculated values could not be obtained. Melting points were recorded in glass capillaries (sealed under nitrogen or argon) and are uncorrected. UV−visible spectra were recorded on a Hitachi 1200 spectrometer. IR spectra were recorded as Nujol mulls between KBr and CsI plates on a Perkin-Elmer 1430 spectrometer.

Synthesis and Characterization of 1−8. (a) Ar′CrCrAr′ (1). A royal-blue solution of $[Ar'Cr(\mu\text{-}Cl)]_2$ (2.11 g, 2.0 mmol) in THF

(9) Cotton, F. A.; Koch, S. A.; Millar, M. *Inorg. Chem.* **1978**, *17*, 2084.
(10) Twamley, B.; Haubrich, S. T.; Power, P. P. *Adv. Organomet. Chem.* **1999**, *44*, 1.
(11) Clyburne, J. A. C.; McMullen, N. *Coord. Chem. Rev.* **2000**, *210*, 73.
(12) Schiemenz, B.; Power, P. P. *Angew. Chem., Int. Ed.* **1996**, *35*, 2150.
(13) Simons, R. S.; Power, P. P. *J. Am. Chem. Soc.* **1996**, *118*, 11966.
(14) Su, J.; Li, X.-W.; Crittendon, C.; Robinson, G. H. *J. Am. Chem. Soc.* **1997**, *119*, 5471.
(15) Olmstead, M. M.; Simons, R. S.; Power, P. P. *J. Am. Chem. Soc.* **1997**, *119*, 11705.
(16) Pu, L.; Senge, M. O.; Olmstead, M. M.; Power, P. P. *J. Am. Chem. Soc.* **1998**, *120*, 12682.
(17) Twamley, B.; Sofield, C. D.; Olmstead, M. M.; Power, P. P. *J. Am. Chem. Soc.* **1998**, *120*, 12682.
(18) Pu, L.; Twamley, B.; Power, P. P. *J. Am. Chem. Soc.* **2000**, *122*, 3524.
(19) Stender, M.; Phillips, A. D.; Wright, R. J.; Power, P. P. *Angew. Chem., Int. Ed.* **2000**, *41*, 1785.
(20) (a) Phillips, A. D.; Wright, R. J.; Olmstead, M. M.; Power, P. P. *J. Am. Chem. Soc.* **2002**, *124*, 5930. (b) Fischer, R. C.; Pu, L.; Fettinger, J. C.; Brynda, M. A.; Power, P. P. *J. Am. Chem. Soc.* **2006**, *128*, 11366.
(21) Wright, R. J.; Phillips, A. D.; Allen, T. L.; Fink, W. H.; Power, P. P. *J. Am. Chem. Soc.* **2003**, *125*, 1694.
(22) Hardman, N. J.; Wright, R. J.; Phillips, A. D.; Power, P. P. *J. Am. Chem. Soc.* **2003**, *125*, 2667.
(23) Nguyen, T.; Sutton, A. D.; Brynda, M.; Fettinger, J. C.; Long, G. J.; Power, P. P. *Science* **2005**, *310*, 844.
(24) Zhu, Z.; Wright, R. J.; Olmstead, M. M.; Rivard, E.; Brynda, M.; Power, P. P. *Angew. Chem., Int. Ed.* **2006**, *45*, 5807.
(25) Zhu, Z.; Fischer, R. C.; Fettinger, J. C.; Rivard, E.; Brynda, M.; Power, P. P. *J. Am. Chem. Soc.* **2006**, *128*, 15068.
(26) Sutton, A. D.; Nguyen, T.; Fettinger, J. C.; Long, G. J.; Power, P. P. *Inorg. Chem.* **2007**, *46*, 4809.
(27) Brynda, M.; Gagliardi, L.; Widmark, P.-O.; Power, P. P.; Roos, B. O. *Angew, Chem., Int. Ed.* **2006**, *45*, 3804.
(28) Stanciu, C.; Richards, A. F.; Stender, M.; Olmstead, M. M.; Power, P. P. *J. Organomet. Chem.* **2006**, *25*, 477.
(29) Wolf, R.; Brynda, M.; Ni, C.; Long, G. J.; Power, P. P. *J. Am. Chem. Soc.* **2007**, *129*, 6076.
(30) Pangborn, A. G.; Giardello, M. A.; Grubbs, R. H.; Rosen, R. K.; Timmers, F. J. *Organometallics* **1996**, *15*, 1518.
(31) Rivard, E.; Fischer, R. C.; Wolf, R.; Yang, P.; Merrill, W. A.; Schley, N.; Zhu, Z.; Pu, L.; Fettinger, J. C.; Teat, S. J.; Novik, I.; Herber, R. H.; Takagi, N.; Nagase, S.; Power, P. P. *J. Am. Chem. Soc.* **2007**, in press.

(25 mL) was added dropwise to a freshly prepared suspension of KC_8 (0.59 g, 4.4 mmol) in THF (10 mL) with cooling in an ice bath. An immediate deep-red color was observed, and stirring was continued for 16 h to ensure complete reduction. The solvent was removed under reduced pressure, and the resulting dark solid was extracted with toluene (40 mL). The solution was filtered, and the deep-red filtrate was concentrated to ca. 15 mL, which afforded deep-red, X-ray-quality crystals of **1**·2PhMe after storage for 2 days at −20 °C. Yield: 0.85 g, 36%. Mp: 200 °C (dec). ^{1}H NMR (300 MHz, C_6H_6, 25 °C): δ 1.11 (br, 12H, CH(CH_3)$_2$), 1.21 (br, 12H, CH(CH_3)$_2$), 1.31 (br, 12H, CH(CH_3)$_2$), 1.83 (br, 12H, CH(CH_3)$_2$), 3.17 (br, 6H, *p*-H of C_6H_3-2,6-^{i}Pr$_2$ and CH(CH$_3$)$_2$), 4.43 (br, 4H, CH(CH$_3$)$_2$), 5.62 (br, 4H, *m*-H of C_6H_3-2,6-^{i}Pr$_2$), 6.93 (br d, 4H, *m*-H of C_6H_3-2,6-^{i}Pr$_2$, $^3J_{HH}$ = 7.5 Hz), ca. 7.1 (2H, *p*-H of C_6H_3-2,6-^{i}Pr$_2$, overlapping with the solvent signal), 7.25 (br, 2H, *m*-H of C_6H_3-2,6-(C_6H_3-2,6-^{i}Pr$_2$)$_2$), 7.45 (br, 2H, *m*-H of C_6H_3-2,6-(C_6H_3-2,6-^{i}Pr$_2$)$_2$); *p*-H of the central aryl ring of C_6H_3-2,6-(C_6H_3-2,6-^{i}Pr$_2$)$_2$ was not observed. UV−vis [hexanes; λ_{max}, nm (ϵ, L mol^{-1} cm^{-1})]: 488 (3200). χ'_M = 0.00112 emu mol^{-1} of Cr between 2 and 320 K.

(b) (4-Me$_3$SiAr′)CrCr(Ar′-4-SiMe$_3$) (2). In a procedure analogous to that used for **1**, [(4-Me$_3$SiAr′)Cr(μ-Cl)]$_2$ (1.6 g, 1.43 mmol) and KC_8 (0.5 g, 3.6 mmol) were reacted to afford a deep-red mixture. After removal of the solvent, the residue was extracted with hexanes (ca. 60 mL). Suitable X-ray-quality crystals of **2** were grown by cooling a saturated toluene solution of **2** at room temperature for several weeks. Yield: 0.17 g, 12%. Mp: 154−157 °C (dark oil). Anal. Calcd for $C_{66}H_{90}Si_2Cr_2$: C, 69.32; H, 7.93. Found: C, 69.51; H, 8.01. ^{1}H NMR (300.08 MHz, C_6D_6, 25 °C): δ 0.47 (s, 18H, SiMe$_3$), 1.13 (br s, 12H, CH(CH_3)$_2$), 1.23 (br s, 12H, CH(CH_3)$_2$), 1.36 (br, 12H, CH(CH_3)$_2$), 1.82 (br, 12H, CH(CH_3)$_2$), 3.13 (br, 6H, *p*-H of C_6H_3-2,6-^{i}Pr$_2$ and CH(CH$_3$)$_2$), 4.44 (br, 4H, CH(CH$_3$)$_2$), 5.63 (br, 4H, *m*-H of C_6H_3-2,6-^{i}Pr$_2$), 6.94 (br d, 4H, *m*-H of C_6H_3-2,6-^{i}Pr$_2$, $^3J_{HH}$ = 7.5 Hz), 7.05 (br tr, 2H, *p*-H of C_6H_3-2,6-^{i}Pr$_2$, $^3J_{HH}$ = 7.5 Hz), 7.41 (br, 2H, *m*-H of the central aryl ring of C_6H_2-2,6-(C_6H_3-2,6-^{i}Pr$_2$)$_2$-4-SiMe$_3$), 7.98 (br, 2H, *m*-H of the central aryl ring of C_6H_2-2,6-(C_6H_3-2,6-^{i}Pr$_2$)$_2$-4-SiMe$_3$). ^{29}Si{^{1}H} NMR (119.16 MHz, C_6D_6, 25 °C): δ −4.02 (s). UV−vis [hexanes; λ_{max}, nm (ϵ, L mol^{-1} cm^{-1})]: 490 (2002). χ'_M = 0.00088 emu mol^{-1} of Cr between 2 and 320 K.

(c) (4-MeOAr′)CrCr(Ar′-4-OMe) (3). A procedure similar to that employed for **2**, using [(4-MeOAr′)Cr(μ-Cl)]$_2$ (1.2 g, 1.15 mmol) and KC_8 (0.34 g, 2.5 mmol), afforded crystals of **3**·2PhMe upon storage of a toluene solution of **3** at −20 °C for 1 day. Yield: 0.24 g, 22%. Mp: 218−220 °C (dark oil). Anal. Calcd for **3**·2PhMe, $C_{76}H_{94}O_2Cr_2$: C, 79.82; H, 8.29. Found: C, 80.62; H, 8.68 (these data suggest some loss of PhMe). ^{1}H NMR (300.08 MHz, C_7D_8, 25 °C): δ 1.13 (br s, 12H, CH(CH_3)$_2$), 1.23 (br s, 12H, CH(CH_3)$_2$), 1.36 (br, 12H, CH(CH_3)$_2$), 1.82 (br, 12H, CH(CH_3)$_2$), 3.19 (br, 6H, *p*-H of C_6H_3-2,6-^{i}Pr$_2$ and CH(CH$_3$)$_2$), 3.69 (s, 6H, OMe), 4.53 (br, 4H, CH(CH$_3$)$_2$), 5.58 (br, 4H, *m*-H of C_6H_3-2,6-^{i}Pr$_2$), 6.90 (br s, 2H, *m*-H of the central aryl ring of C_6H_2-2,6-(C_6H_3-2,6-^{i}Pr$_2$)$_2$-4-OMe), 6.90 (br d, 4H, *m*-H of the central aryl ring of C_6H_2-2,6-(C_6H_3-2,6-^{i}Pr$_2$)-4-OMe, $^3J_{HH}$ = 7.2 Hz), 7.0 (br tr, 2H, p-H of C_6H_3-2,6-^{i}Pr$_2$, overlapping with solvent signals), 7.49 (br, 2H, *m*-H of the central aryl ring of C_6H_2-2,6-(C_6H_3-2,6-^{i}Pr$_2$)$_2$-4-OMe). UV−vis [THF; λ_{max}, nm (ϵ, L mol^{-1} cm^{-1})]: 490 (4500). χ'_M = 0.00150 emu mol^{-1} of Cr between 2 and 320 K.

(d) (4-FAr′)CrCr(Ar′-4-F) (4). Following a procedure similar to that used for **2**, in which [(4-FAr′)Cr(μ-Cl)]$_2$ (1.3 g, 1.3 mmol) and KC_8 (0.38 g, 2.8 mmol) were employed, X-ray-quality crystals of **4**·2PhMe were grown upon storage of a toluene solution of **4** at −20 °C for several days. Yield: 0.23 g, 17%. Mp: 223−225 °C. Anal. Calcd for **4**.2PhMe, $C_{74}H_{88}F_2Cr_2$: C, 79.39; H, 7.92. Found: C, 78.1; H, 7.63 (the data suggest some loss of PhMe). ^{1}H NMR (300.08 MHz, C_7D_8, 21 °C): δ 1.06 (br s, 12H, CH(CH_3)$_2$), 1.18 (br s, 12H, CH(CH_3)$_2$), 1.25 (br, 12H, CH(CH_3)$_2$), 1.82 (br, 12H, CH(CH_3)$_2$), 2.13 (s, CH$_3$ of toluene, overlapping with $C_6D_5CD_2H$), 3.06 (br, 6H, *p*-H of C_6H_3-2,6-^{i}Pr$_2$ and CH(CH$_3$)$_2$), 4.32 (br, 4H, CH(CH$_3$)$_2$), 5.54 (br, 4H, *m*-H of C_6H_3-2,6-^{i}Pr$_2$), 6.70 (br d, 4H, *m*-H of C_6H_3-2,6-^{i}Pr$_2$, $^3J_{HH}$ = 7.2 Hz), 7.57 (br, 2H, *m*-H of the central aryl ring of C_6H_2-2,6-(C_6H_3-2,6-^{i}Pr$_2$)$_2$-4-F); resonances of *m*-H of C_6H_3-2,6-^{i}Pr$_2$ and *m*-H of the central ring of C_6H_2-2,6-(C_6H_3-2,6-^{i}Pr$_2$)$_2$-4-F are not observed because of overlap with solvent signals. ^{19}F{^{1}H} NMR (282.33 MHz, 21 °C): δ −136.7 (br). UV−vis [hexanes; λ_{max}, nm (ϵ, L mol^{-1} cm^{-1})]: 482 (1019). χ'_M = 0.00062 emu mol^{-1} of Cr between 2 and 320 K.

(e) [(4-F$_3$CAr′)Cr(μ-F)(THF)]$_2$ (5). A blue solution of (4-F$_3$-CAr′)CrCl (1.11 g, 20 mmol) in THF was added dropwise to KC_8 (0.29 g, 2.14 mmol) suspended in THF at ca. 0 °C. A deep-red mixture formed and gradually became red-brown upon stirring overnight. The solvent was removed under reduced pressure, and the dark-brown residue was extracted with ca. 50 mL of toluene and filtered. Concentration of the purple-brown filtrate to ca. 15 mL and storage at −20 °C for several days gave large purple crystals of **5**. Yield: 0.10 g, 7%. Mp: 212−214 °C (crystals darken at 88 °C). ^{1}H NMR (300.08 MHz, C_6D_6, 21 °C): δ 1.05 (br s), 2.11 (s, CH$_3$ of toluene), 2.70 (br s), 4.28 (br), 6.90 (s), 7.426 (br s, overlapping with the signal of C_6D_6), 7.57 (br s, overlapping with the signal of C_6D_6). ^{19}F{^{1}H} NMR (282.33 MHz, 25 °C): δ −62.8 (s, CF$_3$), −116.5 (μ-F). UV−vis [THF; λ_{max}, nm (ϵ, L mol^{-1} cm^{-1})]: 538 (90). IR (Nujol): ν (cm^{-1}) 1610 (w), 1600 (w), 1410 (m), 1390 (m), 1345 (m), 1250 (w), 1160 (s), 1018 (w), 998 (m), 945 (m), 870 (m), 855 (m), 790 (m), 763 (w). μ_{eff} = 4.91 μ_B per Cr at 300 K.

(f) [(3,5-^{i}Pr$_2$Ar*)Cr(THF)] (6). A blue solution of (3,5-^{i}Pr$_2$Ar*)-CrCl (0.95 g, 1.46 mmol) in ca. 30 mL of THF was added to a suspension of KC_8 (0.25 g, 1.8 mmol) in THF at 0 °C to give a dark-yellow-orange suspension. Stirring was continued overnight, and the solvent was evaporated. The residue was extracted with ca. 60 mL of hexanes and filtered. The dark-orange filtrate was concentrated to ca. 2 mL and stored at −20 °C for 1 week to afford orange crystals of **2**·*n*-hexane. Yield: 0.22 g, 20%. Mp: 117−119 °C (dec). ^{1}H NMR (300.08 MHz, C_6D_6, 21 °C): δ = 0.5−4 (br), 0.8−1.4 (overlapping m, *n*-hexane), 1.42 (br s, CH_2−CH$_2$O of THF), 3.59 (br s, CH$_2$−CH_2O of THF). UV−vis [hexanes; λ_{max}, nm (ϵ, L mol^{-1} cm^{-1})]: 430 (1100), 628 (400). μ_{eff} = 5.94 μ_B per Cr at 300 K.

(g) [(3,5-^{i}Pr$_2$Ar*)Cr(PMe$_3$)] (7). At ca. 0 °C, a deep-blue solution of (3,5-^{i}Pr$_2$Ar*)CrCl (0.95 g, 1.46 mmol) and PMe$_3$ (0.5 mL, 4.8 mmol) in ca. 40 mL of THF was added to a cold THF suspension of 0.25 g (1.8 mmol) of KC_8. The mixture became deep-orange and was stirred overnight. The solvent was evaporated, and extraction of the residue with hexanes (ca. 60 mL) gave a dark-orange solution upon filtration. Concentration to ca. 5 mL and storage at −20 °C for 2 days gave orange-red crystals of **7**. Yield: 0.20 g, 17%. Mp: 140−141 °C (dec). ^{1}H NMR (300.08 MHz, C_6D_6, 25 °C): δ −1 to +4 (br), 1.23 (br d, $^2J_{PH}$ = 33 Hz), 6.5−10 (br). ^{31}P{^{1}H} NMR (121.5 MHz, C_6D_6, 21 °C): δ 34.3 (s). UV−vis [hexanes; λ_{max}, nm (ϵ, L mol^{-1} cm^{-1})]: 442 (1000), 500 (sh). μ_{eff} = 6.17 μ_B per Cr at 300 K.

(h) [(3,5-^{i}Pr$_2$Ar*)Cr(η^3:η^6-CH$_2$Ph)Cr(Ar*-1-H-3,5-^{i}Pr$_2$)] (8). A blue solution of (3,5-^{i}Pr$_2$Ar*)CrCl (1.28 g, 1.96 mmol) in THF (ca. 40 mL) was added to a suspension of KC_8 (0.28 g, 2.1 mmol, in THF, 10 mL) at 0 °C. A dark-yellow-orange suspension was formed and stirred at ca. 25 °C overnight. The solvent was

evaporated, and toluene (ca. 40 mL) was added. The suspension assumed an olive-green color and, upon storage for 2 days at ca. 25 °C, became dark-red. Filtration, followed by solvent evaporation and extraction with hexanes (ca. 50 mL), afforded a dark-red solution. Concentration to ca. 5 mL and storage at −20 °C gave dark-red crystals of **8**·2.5*n*-hexane. Yield: 0.66 g, 44%. Mp: 208−210 °C (dark oil). ^{1}H NMR (300.08 MHz, C_6D_6, 21 °C): δ 0.8−1.6 (br overlapping m, CH_3 of ^{i}Pr, CH_3, and CH_2 of hexane), 2.6−3.1 (br overlapping m, CH of ^{i}Pr), 4.21 (br d, $^3J_{HH}$ = 5.1 Hz, 2H, *o*-H of $CH_2C_6H_5$), 4.43 (br pseudo-tr, 2H, *m*-H of $CH_2C_6H_5$), 4.47 (br tr, 1H, *p*-H of $CH_2C_6H_5$), 4.66 (s, 2H, $CH_2C_6H_5$), 6.88 (s, aromatic CH), 6.89 (br s, aromatic CH), 6.99 (br s, aromatic CH), 7.33 (s, aromatic CH), 7.42 (br s, aromatic CH), 7.55 (s, aromatic CH), 8.07 (s, aromatic CH). UV−visible [hexanes; λ_{max}, nm (ϵ, L mol^{-1} cm^{-1})]: 346 (11 077), 400−500 (br sh). μ_{eff} = 2.45 μ_B per Cr at 300 K.

Magnetic Measurements. Samples for the magnetic measurements were sealed under vacuum in 4-mm-diameter quartz tubing. Magnetic susceptibilities were measured on a Quantum Design MPMSXL7 superconducting quantum interference device (SQUID) magnetometer. The samples were zero-field-cooled to 2 K, and the magnetization was measured from 2 to 320 K in an applied field of 0.10 or 0.01 T and, in some cases, subsequently from 320 to 2 K. At the lower temperatures, extra elapsed time between measurements ensured that the sample, sealed in a vacuum, was at thermal equilibrium with the temperature sensor. The observed molar magnetic susceptibilities have been corrected for diamagnetic contributions by subtracting −0.000 749, −0.000 738, −0.000 779, −0.000 687, −0.000 907, −0.000 579, −0.000 575, and −0.001 158 emu mol^{-1} for **1**−**8**, respectively, corrections that have been obtained from tables of Pascal's constants. The calculation of the antiferromagnetic exchange coupling constants, when necessary, used the same Hamiltonian as that reported earlier.[26]

X-ray Crystallography. Crystals were removed from a Schlenk tube under a stream of nitrogen and immediately covered with a thin layer of hydrocarbon oil.[32] A suitable crystal was selected, attached to a glass fiber, and quickly placed under a low-temperature nitrogen stream. Data were recorded by using either a Bruker APEX II CCD system (**1**·*n*-hexane, **2**, **5**, and **8**) or a Siemens SMART1000 CCD system (**1**, **3**, and **4**). Absorption corrections were performed using *SADABS*.[33,34] The structures were solved with direct methods, and the non-H atoms were refined anisotropically (except for disordered parts of the molecules, full-matrix least squares on F^2).[35,36]

Computational Studies. Geometry optimizations on the model species (4-XC_6H_4)CrCr(C_6H_4-4-X) (X = H, $SiMe_3$, OMe, and F), in which the bulky terphenyl ligands were replaced with the less computationally expensive para-substituted phenyl derivatives, C_6H_4-4-X, were performed with density functional theory (DFT) methods using the B3LYP functional combined with CRENBL basis sets including the quasi-relativistic pseudopotentials for the Cr atom and a CRENBL basis set for the remaining atoms. To ensure more flexibility, the CRENBL-large orbital basis set with a small core was appended with the polarization functions for C, O, Si, and F. This level of theory is thereafter designated B3LYP/CRENBL. All of the geometry optimizations as well as the determination of the electronic structure were performed with the *Gaussian 03* package.[38] The orbital pictures were generated with the *MOLEKEL* software.[39] An additional set of calculations was performed on the hypothetical Ar*CrCrAr* molecule (Ar* = C_6H_3-2,6-{C_6H_2-2,4,6-^{i}Pr$_3$}$_2$). A nonlocal Perdew correlation in combination with the VWN5 local correlation, as well as basis sets of triple-ζ quality with a polarization function (TZP), was used to optimize the geometry of the Ar*CrCrAr* species, as implemented in ADF code.[40] Relativistic effects were taken into account using the full-electron zero-order regular approximation (ZORA) to the electronic Hamiltonian,[41] hereafter described as TZP/BVP86/ZORA. The geometry optimizations and single-point calculations on the model species (2,6-$Ph_2C_6H_3$)ArCr(L) (L = PMe_3 or THF), [(2,6-Ph_2-4-$F_3CC_6H_2$)Cr(μ-F)(THF)]$_2$, and [(2,6-$Ph_2C_6H_3$)Cr(η^3:η^6-CH_2Ph)Cr(C_6H_3-2,6-$Ph_2C_6H_3$)] were performed at the B3LYP/6-31g* level, using the *Gaussian 03* package.[38]

Results

Syntheses and Characterization of the Chromium(I) Dimers ArCrCrAr (1−4; Ar = C_6H_2-2,6-(C_6H_3-2,6-^{i}Pr$_2$)$_2$-4-X, Where X = H, $SiMe_3$, OMe, and F). Compounds **1**−**4** were synthesized in moderate yields by the reduction of the divalent precursors ArCrCl[26] with a slight excess of KC_8 in THF (Scheme 1). Very air-sensitive, deep-red crystals of **1**−**4** were obtained from either toluene or *n*-hexane solutions. Their low-temperature X-ray crystal structures (Table 1) revealed similar trans-bent dimeric structures with short Cr−Cr distances ranging from 1.8077(7) to 1.8351(4) Å (Figure 1and Table 2). Compounds **1**−**3** reside on a crystallographic inversion center, but this is not the case for **4**, which shows a slightly twisted arrangement of the C(ipso)CrCrC(ipso) core (C1−Cr1−Cr2−C31 = 172.8°). The C(ipso)−Cr−Cr angles in **1**−**4** remain almost unchanged and in the narrow range 101.65(6)−102.78(1)°. A notable feature of the structures is the close approach of one of the C_6H_3-2,6-^{i}Pr$_2$ substituents of each terphenyl ligand to one of the Cr^I ions. The Cr−C(ipso) distances of the interacting flanking aryl rings range from 2.294(1) to 2.322(2) Å, and the remaining Cr−C distances exceed 2.41 Å.

The UV−visible spectra of **1**−**4** display intense absorptions below 250 nm, as well as a less intense absorption maximum in the narrow range from 482 to 490 nm. The ^{1}H NMR spectra of **1**−**4** also display little variation: At room

(32) Hope, H. *Prog. Inorg. Chem.* **1995**, *41*, 1.
(33) Blessing, R. H. *Acta Crystallogr.* **1995**, *51A*, 33.
(34) Sheldrick, G. M. *SADABS, Siemens Area Detector Absorption Correction*, version 2.10; Universität Göttingen: Göttingen, Germany, 2003. Sheldrick, G. M. (personal communication) *TWINABS: An Empirical Correction for Absorption Anisotropy applied to Twinned crystals*, version 1.05; Universität Göttingen: Göttingen, Germany, 2003.
(35) Sheldrick, G. M. *SHELXTL*, version 6.1; Bruker AXS, Inc.: Madison, WI, 2002.
(36) Sheldrick, G. M. *SHELXS97 and SHELXL97*; Universität Göttingen: Göttingen, Germany, 2002.
(37) Sheldrick, G. M. (personal communication) *CELLNOW, Twin matrix determination program*; Universität Göttingen: Göttingen, Germany, 2003.
(38) Frisch, M. J.; et al. *Gaussian 03*, revision A.1; Gaussian, Inc.: Pittsburgh, PA, 2003.
(39) Flukiger, P.; Luthi, H. P.; Portmann, S.; Weber, J. *MOLEKEL 4.3*; Swiss Center for Scientific Computing: Manno, Switzerland, 2000−2002.
(40) (a) te Velde, G.; Bickelhaupt, F. M.; van Gisbergen, S. J. A.; Fonseca Guerra, C.; Baerends, E. J.; Snijders, J. G.; Ziegler, T. *J. Comput. Chem.* **2001**, *22*, 931. (b) Fonseca Guerra, C.; Snijders, J. G.; te Velde, G.; Baerends, E. J. *Theor. Chem. Acc.* **1998**, *99*, 391. (c) Bearends, E. J.; et al. *ADF2006.01*; SCM, Theoretical Chemistry, Vrije Universiteit: Amseterdam, The Netherlands. http://www.scm.com.
(41) van Lenthe, E.; Ehlers, A. E.; Baerends, E. J. *J. Chem. Phys.* **1999**, *110*, 8943.

Table 1. Crystallographic Data for **2**−**5** and **8**

	2	**3**·2PhMe	**4**·2PhMe	**5**·2PhMe	**8**·2.5*n*-hexane
empirical formula	$C_{66}H_{90}Cr_2Si_2$	$C_{62}H_{78}O_2Cr_2{\cdot}2C_7H_8$	$C_{60}H_{72}F_2Cr_2{\cdot}2C_7H_8$	$C_{70}H_{88}O_2F_8Cr_2{\cdot}2C_7H_8$	$C_{91}H_{130}Cr_2{\cdot}2.5C_6H_{14}$
M	1043.56	1143.51	1027.31	1401.67	1543.38
T, K	90(2)	90(2)	90(2)	90(2)	90(2)
cryst syst	triclinic	triclinic	triclinic	triclinic	triclinic
space group	$P\bar{1}$	$P\bar{1}$	$P\bar{1}$	$P\bar{1}$	$P\bar{1}$
a/Å	11.6752(4)	10.2466(8)	9.822(2)	9.8443(5)	19.011(2)
b/Å	12.0201(4)	11.1972(9)	13.937(3)	13.8545(7)	19.075(2)
c/Å	12.4185(4)	15.207(2)	20.835(4)	14.2731(8)	26.796(2)
α/deg	94.827(1)	109.655(2)	106.625(4)	101.999(1)	90.915(1)
β/deg	114.882(1)	92.661(2)	93.504(4)	98.780(1)	93.208(1)
γ/deg	96.952(1)	105.614(2)	94.576(4)	93.103(1)	90.861(1)
V/Å^3	1551.62(9)	1564.3(2)	2713.6(9)	1874.4(2)	9699(2)
Z	1	1	2	1	4
ρ_{calcd}/Mg m^{-3}	1.117	1.214	1.257	1.242	1.057
θ_{max}/deg	25.66	30.03	25.25	29.60	27.48
total data	17 987	23 869	9794	14 994	125 305
unique data (R_{int})	5869	9062	7896	6037	44364
param (restraints)	496 (0)	549 (0)	658 (42)	617 (0)	1974 (69)
GOF on F^2	1.005	0.951	0.894	0.842	1.021
R1, wR2 [$I > 2\sigma(I)$]	0.0382 (0.0813)	0.0420 (0.1027)	0.0660 (0.1844)	0.0476 (0.1233)	0.0758 (0.1808)
R1, wR2 (all data)	0.0591 (0.0895)	0.0635 (0.1162)	0.0866 (0.1933)	0.0616 (0.1311)	0.1035 (0.1966)
largest diff peak and hole/e Å^{-3}	0.403 and −0.284	0.892 and −0.446	0.903 and −0.994	0.943 and −0.241	0.902 and −0.554

Scheme 1. Syntheses of **1**−**8**

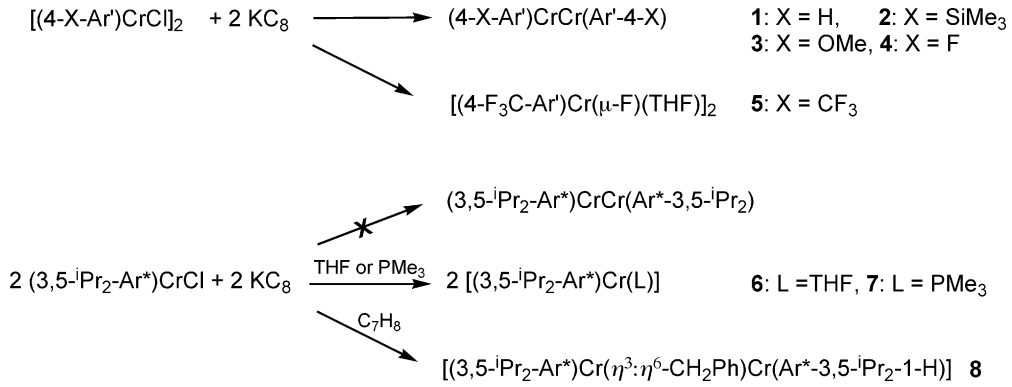

temperature, broadened signals were observed because of their weak paramagnetism or because of the fluxional behavior of the terphenyl substituents. At low temperatures, the spectra displayed sharper signals, although the general features of the spectra remained unchanged. The ^{1}H NMR spectrum of (4-MeOAr′)CrCr(Ar′-4-OMe) (**3**; Figure 2) is representative of the four complexes and includes four diastereotopic methyl resonances, one signal for the MeO group, as well as two signals for the protons in the meta postions of the flanking aryl ligand. The multiplets at 3.21 and 4.62 ppm correspond to tertiary CH resonances of the ^{i}Pr groups. The spectrum is consistent with C_{2h} symmetry and the presence of two inequivalent flanking C_6H_3-2,6-^{i}Pr$_2$ substituents due to restricted rotation about the Cr−C(ipso) bond (Figure 1). An unusual feature of the spectrum is the dramatically shielded signal of the *p*-H atom of one of the flanking aryl rings. The signal for the corresponding *m*-H atoms is also shifted to lower frequency. This observation is explained by the proximity of the respective H atoms to a flanking aryl ring of the opposite terphenyl ligand, which induces a diamagnetic shift of these resonances. These signals may be assigned to the flanking ring closest to the Cr atom.

The molar magnetic susceptibilities of **1**−**4** were measured at an applied field of 0.01 or 0.1 T after zero-field cooling to 2 K. The results for **2** and **4** are shown in Figures 3 and 4. Similar results for **1** were reported earlier.[23] For **1**−**4**, the corrected molar magnetic suceptibility, χ'_M, is very small and is composed of three components. The only component associated directly with **1**−**4**, which are essentially fully exchange coupled $3d^5-3d^5$ Cr^I-Cr^I dimers, is the second-order Zeeman contribution to the susceptibility. This so-called "temperature-independent paramagnetism" (TIP) results from a second-order perturbation mixing of the fully spin-coupled ground state with the various Boltzmann-depopulated paramagnetic excited states. The magnetism arising from TIP is shown in red in Figures 3 and 4 and has values of 0.00112(5), 0.00088(3), 0.00150(10), and 0.00062(3) emu mol^{-1} of Cr for compounds **1**−**4**, respectively. The remaining two χ'_M components result from the presence of traces of isolated paramagnetic $3d^4$ Cr^{II} with an assumed magnetic moment of 4.90 μ_B (denoted in blue) and traces of weakly exchange-coupled $Cr^{II}Cr^{II}$ dimers (denoted in green). The amount of these trace impurities corresponds to 3.0, 1.6, ca. 0.6, and 0.48 wt % Cr^{II} in **1**−**4**, respectively.

Calculations for Model Complexes of 1−**4.** The overall trend in the computed geometries obtained from DFT calculations on (4-XC_6H_4)CrCr(C_6H_4-4-X) (X = H, $SiMe_3$, OMe, and F) models broadly agrees with the experimental

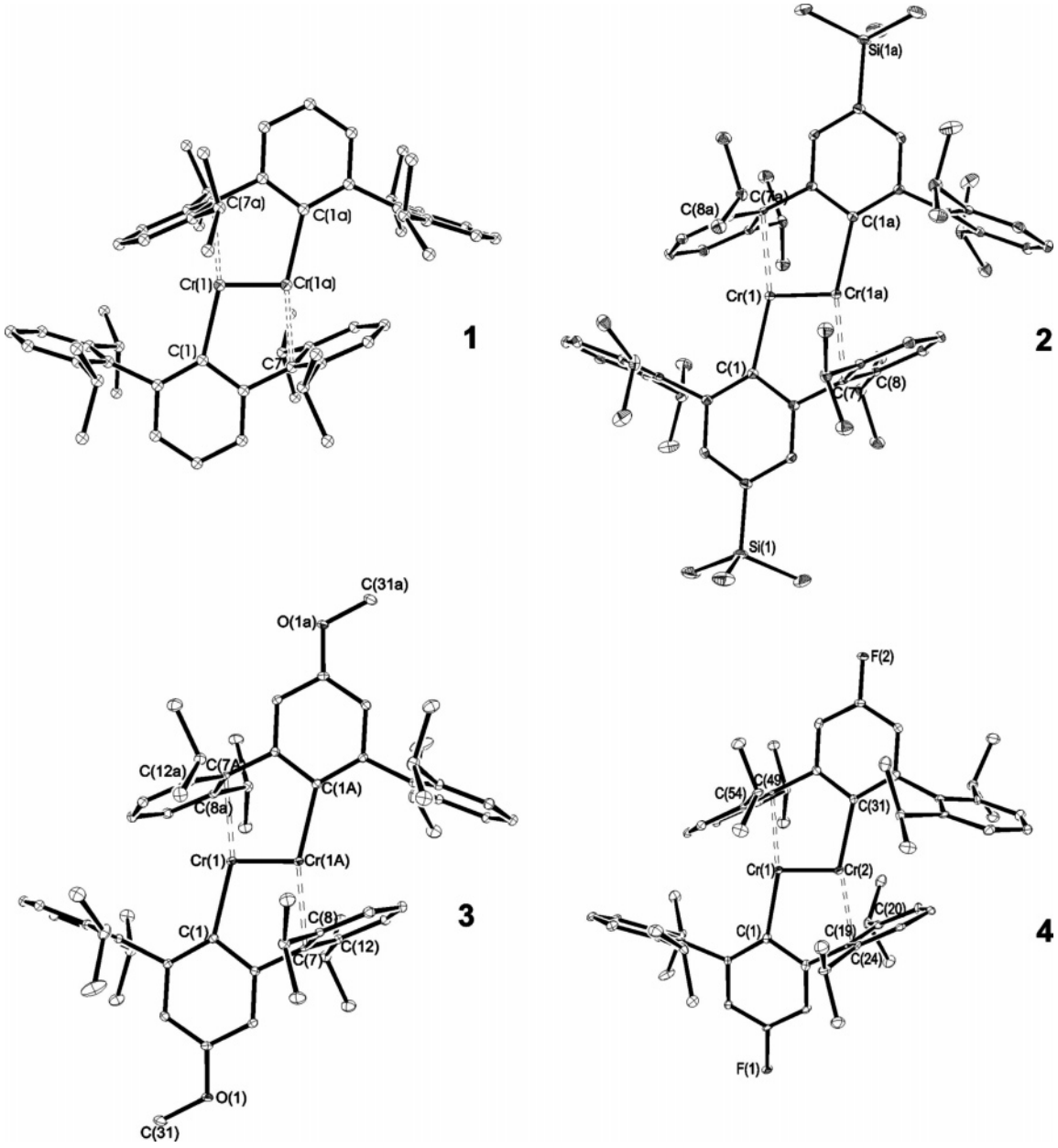

Figure 1. Solid-state molecular structures of **1**−**4** (30% thermal ellipsoid level; the solvent molecules and H atoms are not shown for clarity).

Table 2. Selected Bond Lengths (Å) and Angles (deg) of **1**−**4**

	1	**2**	**3**		**4**
Cr1−Cr1a	1.8351(4)	1.8077(7)	1.8160(5)	Cr1−Cr2	1.831(2)
Cr1−C1	2.131(1)	2.136(2)	2.131(2)	Cr1−C1, Cr2−C31	2.132(6), 2.138(6)
Cr1−C7a	2.294(1)	2.322(2)	2.311(2)	Cr1−C49, Cr2−C19	2.307(6), 2.294(6)
C1−Cr1−Cr1a	102.78(1)	101.65(6)	102.25(4)	Cr1−Cr2−Cr31, Cr1−Cr2−Cr1	102.7(2) 102.3(2)
C7−Cr1a−Cr1	94.19(3)	95.73(5)	95.37(4)	C19−Cr2−Cr1, C49−Cr1−Cr2	94.6(2), 94.3(2)
C1−Cr1−Cr1a−C1a	180.0	180.0	180.0	C1−Cr1−Cr2−C31	172.8

ones. However, the metal−metal distances calculated for the model species are shorter because of lower steric effects and the absence of interactions between the flanking ring and the metal. The changes in the Cr−Cr bond lengths and the C−Cr−Cr bond angles are small (within 0.009 Å for the Cr−Cr bond length and 3.1° for the Cr−Cr−C angle; Table 3 and Figure S1 of the Supporting Information). In order to assess the influence of the steric bulk of the flanking aryl rings in the terphenyl ligand, we also optimized the structure of the bulky Ar*CrCrAr* species (Ar* = C_6H_3-2,6-{C_6H_2-2,4,6-$^iPr_3$}$_2$) at the TZP/BVP86/ZORA level of theory. The optimized CCrCrC core parameters differ only slightly from those of (2,6-$Ph_2C_6H_3$)CrCr(C_6H_3-2,6-Ph_2) and **1** that we reported in our recent publications (Table 4 and Figure S2 of the Supporting Information).[23,27] Inspection of Table 4 clearly shows that increasing the size of the ligand from Ph to 2,6-$Ph_2C_6H_3$, Ar′, or Ar* affords an elongation of the Cr−Cr bond. This elongation is accompanied by an opening of

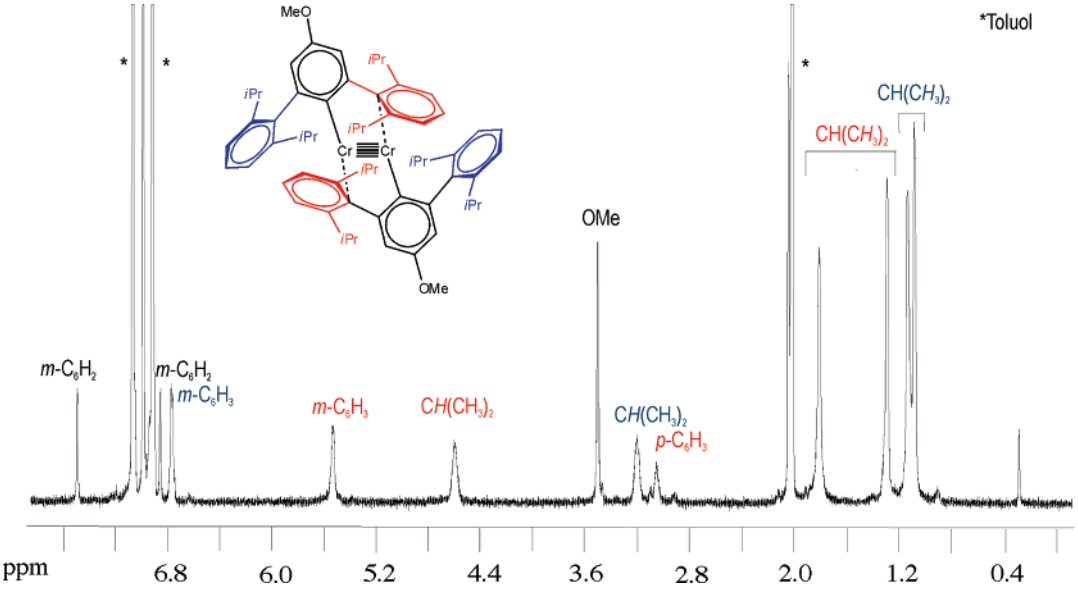

Figure 2. ^{1}H NMR spectrum of **″3** in C_7D_8 at −50 °C (asterisks denote signals of the solvent toluene).

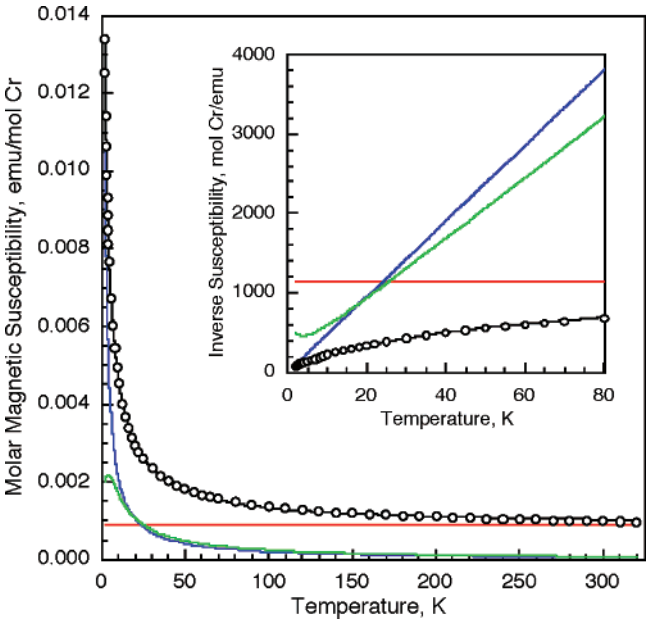

Figure 3. Plot of the molar magnetic susceptibility of **2** vs temperature, obtained in a 0.01 T applied field. The open circles are the observed molar magnetic susceptibility, χ'_M, the black line is the sum of the temperature-independent susceptibility of **2**, red line, and the sum of trace impurities arising from paramagnetic chromium(II) with a μ_{eff} of 4.90 μ_B, blue line, and exchange-coupled chromium(II) dimers with a J of −0.63 cm^{-1}, green line. Inset: Plot of the corresponding inverse molar magnetic susceptibility, $1/\chi'_M$, of **2** obtained between 2 and 80 K.

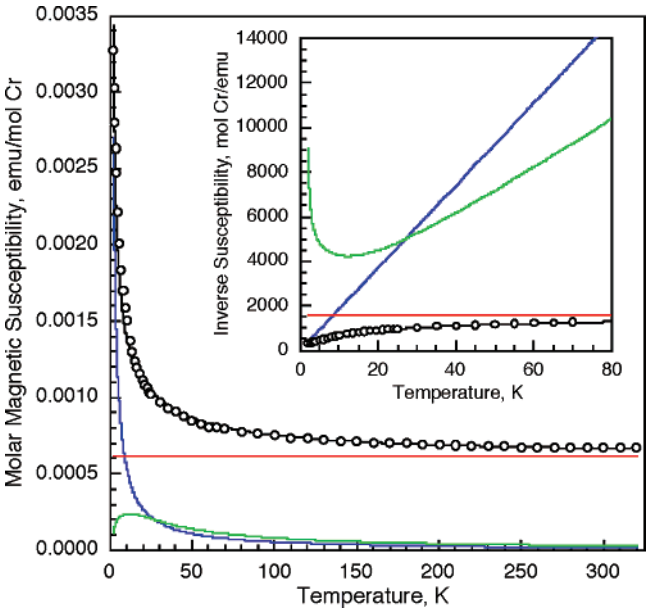

Figure 4. Plot of the molar magnetic susceptibility of **4**, obtained in a 0.1 T applied field, vs temperature. The open circles are the observed molar magnetic susceptibility, χ'_M, and the black line is the sum of the temperature-independent susceptibility of **4**, red line, and the sum of trace impurities arising from paramagnetic chromium(II) with a μ_{eff} of 4.90 μ_B, blue line, and exchange-coupled chromium(II) dimers with a J of −2.0 cm^{-1}, green line. Inset: Plot of the corresponding inverse molar magnetic susceptibility, $1/\chi'_M$, of **4** obtained between 2 and 80 K.

the C(ipso)−Cr−C angle and the increasing difference between the C1−C(ipso)−Cr and C2−C(ipso)−Cr angles. Further inspection of the optimized geometries species reveals that the flanking aryl rings bend away from the CCrCrC core in the hypothetical Ar*CrCrAr* molecule, in comparison to the less bulky Ar′CrCrAr′ and ArCrCrAr species. This is demonstrated by the substantial increase of the distance between the Cr center and the *para*-C atom of the flanking aryl [Cr−C (para) distances range from 3.29 to 3.51 Å; see Table 4]. Furthermore, short contacts are observed between the CH moiety of the *p*-^{i}Pr group of one flanking 2,4,6-^{i}Pr$_3$C$_6$H$_2$ ring and the meta and para ring C atoms of a flanking 2,4,6-^{i}Pr$_3$C$_6$H$_2$ group from the Ar* ligand on the other Cr (the C−H distances range from 2.559 to 2.797 Å and the C−C distances from 3.614 to 3.722 Å).

Restricted DFT calculations indicate that the Cr−Cr bond in **1** and its simplified models are quintuple in nature.[23,27] In order to see how the changes in the electronic structure of the ligands affect the bonding in the Cr−Cr fragment, we have also analyzed the electronic structures of the optimized models as well as of the experimentally determined geometries of **1**−**4**. Calculations analogous to those reported earlier for **1** were used to analyze the species exhibiting the

Table 3. Comparison of Key Bond Lengths (Å) and Angles (deg) of the Model Compounds (4-XC_6H_4)CrCr(C_6H_4-4-X) (X = H, $SiMe_3$, OMe, and F) Optimized at the B3LYP/CRENBL Level of Theory with Experimental Values from the Solid-State Structures of ArCrCrAr (Ar = **1**−**4**; Ar = C_6H_2-2,6-(C_6H_3-2,6-$^iPr_2$)-4-X, X = H, $SiMe_3$, OMe, and F)[a]

	(4-XC_6H_4)CrCr(C_6H_4-4-X)			ArCrCrAr	
X	CrCr	C(ipso)Cr	CCrCr	CrCr	CCrCr
H	1.660	2.024	95.2	1.835	102.8
$SiMe_3$	1.660 (0.000)	2.023 (−0.001)	96.0 (0.8)	1.808 (−0.035)	101.7 (−0.9)
OMe	1.662 (0.002)	2.015 (−0.009)	98.3 (3.1)	1.816 (−0.019)	102.3 (−0.5)
F	1.660 (0.000)	2.023 (−0.001)	97.3 (2.1)	1.831 (−0.004)	102.7 (−0.1), 102.3 (−0.5)

[a] Differences of the substituted derivatives to the parent species PhCrCrPh and Ar′CrCrAr′, respectively (X = H), are given in parentheses.

Table 4. Geometrical Parameters of the CCrCrC Cores Obtained from the DFT-Optimized PhCrCrPh, (2,6-$Ph_2C_6H_3$)CrCr(C_6H_3-2,6-Ph_2), Ar′CrCrAr′, and Ar*CrCrAr* Species at the TZP/BVP86/ZORA Level of Theory[a]

ligand	CrCr	C(ipso)CrCr	C1C(ipso)Cr	C2C(ipso)Cr	$CrC^{(Fl)}$(ipso)	$CrC^{(Fl)}$(para)
Ph	1.684	92.9	120.0	123.9		
2,6-$Ph_2C_6H_3$	1.725	102.2	114.7	130.7	2.303	3.286
Ar′	1.725	102.5	114.1	131.5	2.282	3.288
Ar*	1.721	103.8	111.9	133.8	2.277	3.505
Ar′, expt for **1**	1.835	102.7	114.4	131.7	2.294	2.996

[a] The experimental parameters for the Ar′CrCrAr′ (**1**) are also included for comparison. $C^{(Fl)}$(ipso) stands for the *ipso*-C atom of the flanking aryl ring displaying a secondary interaction with Cr; $C^{(Fl)}$(para) stands for the *p*-C atom of the same flanking aryl ring.

modified ligands used in this work. The resulting molecular orbitals and calculated bond orders of all of the species studied here are virtually the same as those for **1** and, therefore, will not be discussed further.

Synthesis and Characterization of 5. The reaction of (4-F_3CAr′)CrCl with KC_8 was carried out analogously to the syntheses of **1**−**4** to prepare the metal−metal-bonded dimer (4-F_3CAr′)CrCr(Ar′-4-CF_3) (Scheme 1). Initially, the reaction mixture assumed the deep-red color seen for the other ArCrCrAr complexes; however, the color soon changed to dark brown, suggesting that some decomposition had occurred. After removal of the solvent and extraction with toluene, purple crystals of **5** were isolated.

The molecular structure of **5** (Figure 5)[42] shows a centrosymmetric arrangement of quasi-square-planar Cr^{II} cations connected by two μ_2-bridging fluorides with a Cr−Cr separation of 3.109(2) Å. The planar Cr_2F_2 core has differing Cr−F distances [Cr1−F1 and Cr1−F1a = 1.970(2) and 2.104(2) Å, respectively]. The coordination sphere of the Cr atoms is completed by η^1-bound 4-F_3CAr′ and THF ligands. The observed magnetic susceptibility between ca. 20 and 330 K corresponds to that expected for an antiferromagnetically exchange-coupled Cr^{II}−Cr^{II} dimer, with a fitted coupling constant, *J*, of −2.5 cm^{-1} and a 2.5 wt % trace of a paramagnetic monomeric Cr^{II} impurity with a spin-only μ_{eff} of 4.90 μ_B. A deviation observed below ca. 20 K is probably the result of a small zero-field splitting of the ground state of the Cr^{II} ion produced by the very low symmetry of the coordination environment. The ^{1}H NMR spectrum of **5** showed extremely broad signals. A singlet at −62.8 ppm and a broad peak at −116.5 ppm in the $^{19}F\{^1H\}$ NMR spectrum in C_6D_6 may be assigned to the ligand CF_3 group and the bridging F atoms, respectively. The UV−visible spectrum in hexanes showed an extremely broad, weak maximum at 538 nm. No O−H stretch was observed in the IR spectrum.

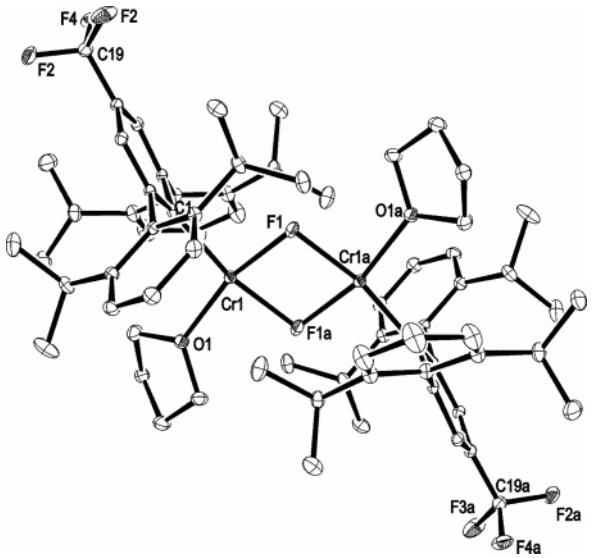

Figure 5. Solid-state molecular structure of **5** (30% thermal ellipsoid level; the H atoms and solvent toluene are not shown for clarity). Selected bond distances (Å) and angles (deg): Cr1−C1 2.117(2), Cr1−F1 1.970(2), Cr1−F1a 2.104(2), Cr1−O1 2.052(2), Cr1−Cr1a 3.109(2), F1−Cr1−F1a 77.89(6), Cr1−F1−Cr1a 102.11(7), F1−Cr1−C1 92.15(6), O1−Cr1−F1a 88.17(6).

A molecular orbital analysis was performed with the μ-fluoro-bridged model species [(2,6-Ph_2-4-$F_3CC_6H_2$)Cr(μ-F)(THF)]$_2$ using single-point B3LYP/6-31g* calculations using the geometry of **5** obtained from the crystal structure. The highest occupied molecular orbital (HOMO) to HOMO−3 orbitals are similar in that they are mainly composed of the two almost pure d metal orbitals, slightly distorted from the Cr−Cr axis by the nearby O atoms from the THF molecules (see Figure S3 of the Supporting Information).

Syntheses and Characterization of 6−**8.** The monomeric complexes **6** and **7** were obtained in moderate yields as air-

(42) The possibility that **5** was a hydroxide of the composition [4-F_3CAr′)Cr(μ-OH)(THF)$_2$ was also entertained. This cannot be excluded on the basis of the Cr−X distances (X = O vs F); however, replacing the bridging F atoms with O led to a significantly worse final refinement of the crystal structure. Furthermore, no O−H stretch was observed in the IR spectrum of **5**, and the synthesis was reproducible when air and moisture were carefully excluded.

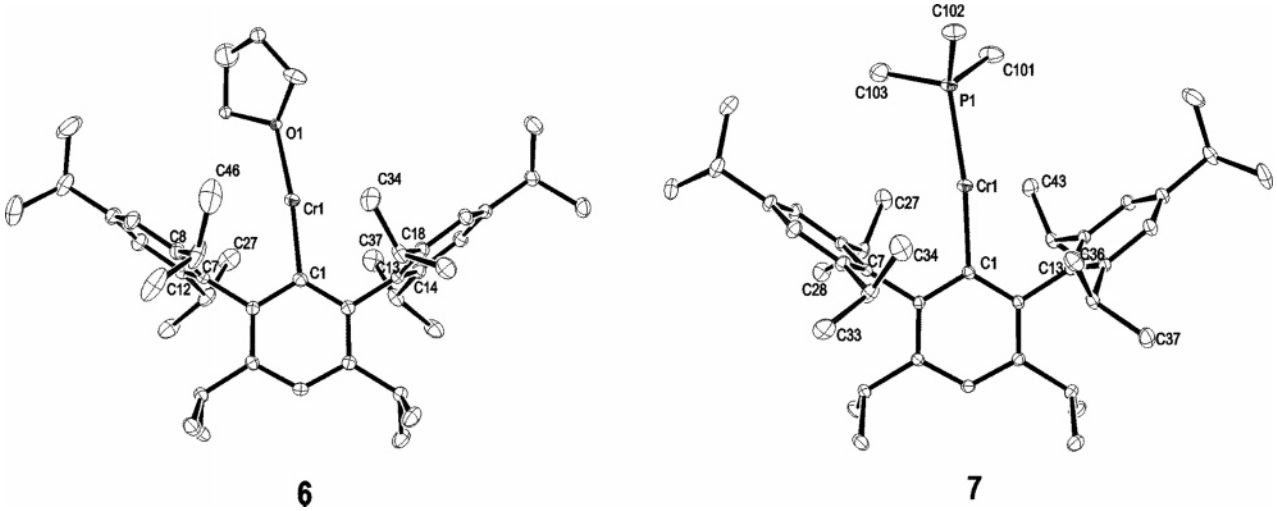

Figure 6. Solid-state molecular structures of **6** and **7** (30% thermal ellipsoid level; the H atoms are not shown; hexane solvent molecule and disorder in the THF molecule of **6** are not shown for clarity).

Table 5. Selected Bond Lengths (Å) and Angles (deg) of **6** and **7**

	6	**7**
Cr1−O1/Pl	2.062(5)	2.4646(4)
Cr1−C1	2.087(3)	2.116(2)
Cr1−C7	3.041(3)	3.136(3)
Cr1−C13	3.361(3)	3.279(2)
Cr1−C27,C34, C37,C46	3.744(4)−4.141(4)	3.674(2)−4.396(1)
O1−Cr1−C1, P1−Cr1−C1	173.7(2)	167.39(4)

sensitive orange (**6**) or orange-red (**7**) crystals from the reaction of (3,5-^{i}Pr$_2$Ar*)CrCl with KC_8 in THF and THF/PMe_3, respectively. Dark-red crystals of **8** were isolated in 44% yield after treatment of the crude reaction product with toluene, followed by recrystallization from hexanes (Scheme 1). The molecular structures of **6** and **7** (Figure 6 and Table 5) show that the Cr atoms have a nearly linear geometry [**6**, O1−Cr1−C1 = 173.7(2)°; **7**, P1−Cr1−C1 = 167.39(4)°]. The Cr−C(ipso) distance in **7** [Cr1−C1 = 2.116(2) Å] is slightly longer than that in **6** [Cr1−C1 = 2.087(3) Å], while all other C−Cr contacts are longer than 3.0 Å.

In the X-ray crystal structure of **8** (see Figure 7), the asymmetric unit contains two molecules of the binuclear **8** that have very similar geometries. Both crystallographically independent molecules of **8** show some degree of disorder, and we focus our discussion on the less disordered molecule. One chromium, Cr1, is σ-bound to an anionic (3,5-^{i}Pr$_2$Ar*)$^-$ ligand via the C(ipso) of its central aryl ring [Cr1−C101 = 2.051(3) Å], supplemented by a longer interaction with the C(ipso) of one of the flanking aryl rings [Cr1−C113 = 2.474(3) Å]. Cr1 is also bound to three C atoms of the benzylic segment of the anion [Cr1−C1, Cr1−C2, and Cr1−C7 = 2.279(3), 2.407(3), and 2.098(3) Å, respectively]. The other chromium, Cr2, is bound to both the phenyl ring of the benzyl anion and the encapsulated flanking aryl ring of a 3,5-^{i}Pr$_2$Ar*-1-H ligand, each in an η^6-fashion [Cr2−centroid distances = 1.626 Å (Ph) and 1.664 Å (2,4,6-^{i}Pr$_3$C$_6$H$_2$); centroid−Cr2−centroid angle = 174.3°].

Characterization of **6**−**8** by ^{1}H NMR spectrocopy was complicated by their paramagnetism and, in the cases of **6** and **7**, by their instability in a C_6D_6 solution. Dissolution of **6** in deuterated benzene immediately gave a dark-green solution, and the ^{1}H NMR spectrum showed the signals of free THF along with an extremely broad signal at 0.5−4 ppm. When the solution was stored at ca. 25 °C for several days, the color slowly changed to yellow. After 1 week, numerous signals consistent with the presence of several distinct chemical environments for the ^{i}Pr and aryl groups of the ligands were present. The PMe_3 complex **7** initially formed an orange solution in C_6D_6, and the ^{1}H NMR spectrum displayed two extremely broad peaks at −1 to +4 and 6.5−10 ppm as well as a doublet at 1.23 ppm due PMe_3 methyl groups. The ^{31}P{^{1}H} NMR spectrum of **7** afforded a signal at +34 ppm. After standing for 1 day at room

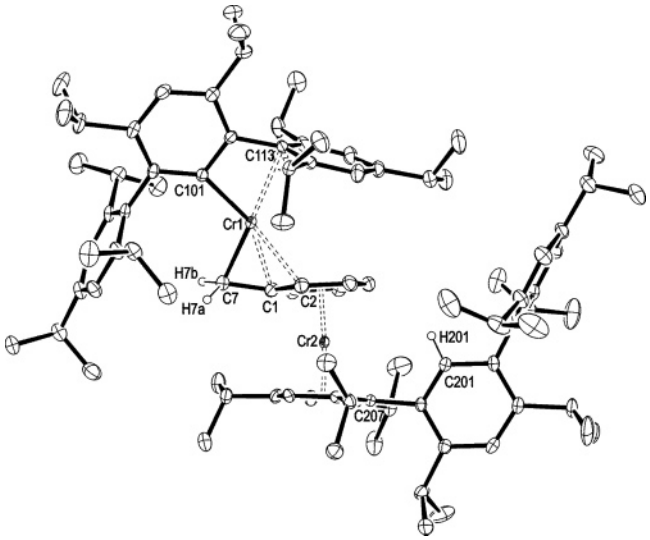

Figure 7. Solid-state molecular structure of **8** (30% thermal ellipsoid level). Only one of the two crystallographically independent molecules of **8** is shown; hexane solvent molecules, H atoms (except H51), and disorder in one of the flanking C_6H_2-2,4,5-^{i}Pr$_3$ groups are not shown for clarity. Selected bond distances (Å) and angles (deg): Cr1−C101 2.051(3), Cr1−C113 2.474(3), Cr1−C1 2.279(3), Cr1−Cr2 2.407(3), Cr1−C7 2.098(3), Cr2−centroid 1.626 (Ph) and 1.664 (2,4,6-^{i}Pr$_3$C$_6$H$_2$), C1−C7 1.459(4), C101−Cr1−C7 111.9(1), C101−Cr1−C1 147.6(1), C101−Cr1−C2 168.95(1), C7−Cr1−C113 174.06(1), C7−C1−centroid 169.3, centroid−Cr2−centroid 174.3.

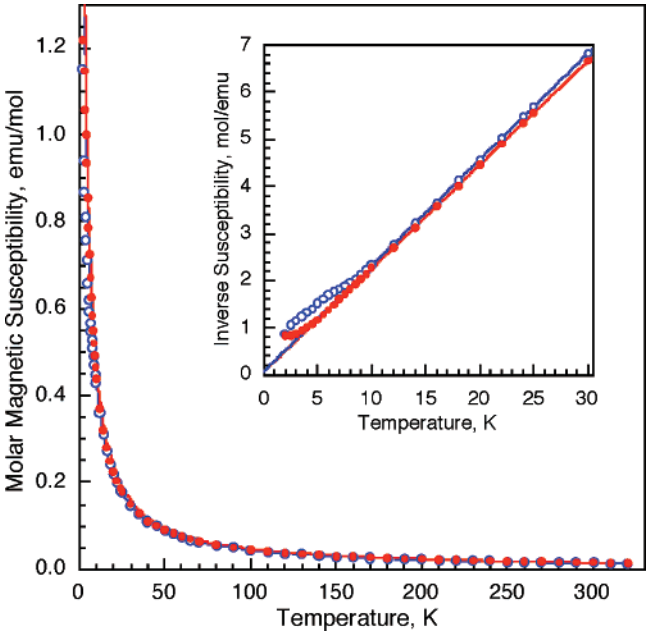

Figure 8. Plot of the molar magnetic susceptibilities vs temperature of **6**, blue open points, and **7**, red points, obtained in a 0.01 T applied field. The points are the observed molar magnetic susceptibilities, χ'_M, and the lines are the χ'_M values that correspond to paramagnetic chromium(I) compounds with μ_{eff} values of 5.96 and 6.17 μ_B for **6** and **7**, respectively. Inset: Plot of the corresponding inverse molar magnetic susceptibilities, $1/\chi'_M$, of **6** and **7** obtained between 2 and 30 K.

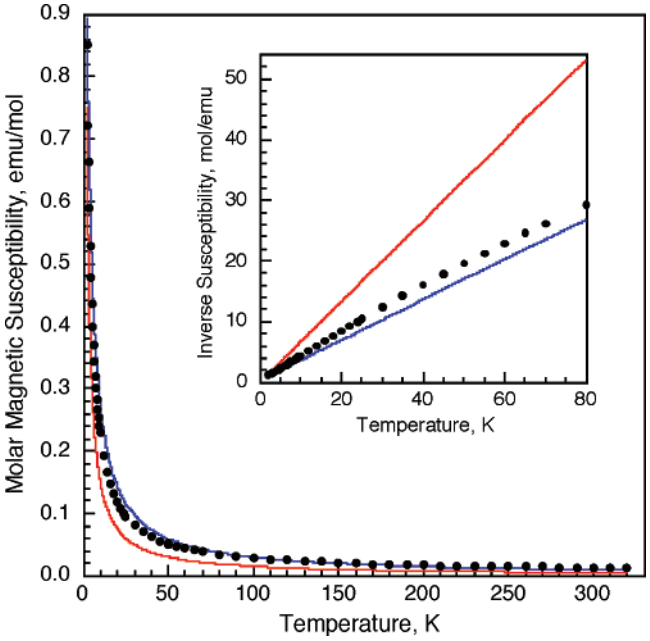

Figure 9. Molar magnetic susceptibility of **8**, obtained in a 0.01 T applied field. The solid circles are the observed molar magnetic susceptibility, χ'_M, and the red line is the χ'_M that corresponds to paramagnetic chromium(II) with μ_{eff} = 4.90 μ_B. The blue line is the χ'_M that corresponds to an antiferromagnetic exchange-coupled chromium(II)−chromium(II) dimer with J = −0.15 cm^{-1}. Inset: Corresponding inverse molar magnetic susceptibility, $1/\chi'_M$, of **8** obtained between 2 and 80 K.

temperature, this solution had become olive-green and numerous signals were observed in the ^{1}H NMR spectrum, indicating a decomposition similar to that observed in **6**. The ^{1}H NMR spectrum of **8** in C_6D_6 was also very complex. Nevertheless, characteristic signals at 4.21, 4.43, 4.47, and 4.66 ppm (intensity ratio 2:2:1:2) can be assigned to the Cr-bound benzyl anion.

The UV−visible spectra of **6** and **7** in hexanes contained moderately intense absorptions at 430 nm (**6**) and 442 nm (**7**). An additional absorption maximum was observed for **6** at 628 nm, whereas a broad shoulder was observed for **7** at around 500 nm. The UV−visible spectrum of **8** showed an intense maximum at 346 nm and a very broad shoulder at 400−500 nm.

The magnetic properties of **6** and **7** (Figure 8), obtained in an applied field of 0.01 T, are very similar. As is shown in the inset, a plot of inverse molar magnetic susceptibility, $1/\chi'_M$, vs T of **6** is linear above 10 K, and its slope yields a Curie constant, C, of 4.441(5) emu K mol^{-1}, a Weiss temperature, Θ, of −0.75(2) K, and a corresponding μ_{eff} of 5.96 μ_B. As shown in the inset to Figure 9, the observed $1/\chi'_M$ vs T of **7** is linear above 7 K, and its slope yields a C of 4.769(4) emu K mol^{-1}, a Θ of −1.82(2) K, and a corresponding μ_{eff} of 6.17 μ_B. In Figure 9, the observed magnetic susceptibility of **8** is most consistent with the presence of very weak $3d^4-3d^4$ antiferromagnetic exchange with a coupling constant, J, of −0.15 cm^{-1}. However, the possible presence of Cr^{II} zero-field splitting may yield fits that are consistent with the absence of any exchange coupling, i.e., with fully paramagnetic Cr^{II}.

Geometry optimizations of the model species [(2,6-$Ph_2C_6H_3$)Cr(THF)] and [(2,6-$Ph_2C_6H_3$)Cr(PMe_3)] at the B3LYP/6-31g* level of theory in the high-spin sextet state reproduced the geometries of **6** and **7** fairly well. Molecular orbital analysis showed that five half-occupied d orbitals of Cr form the five HOMOs of both **7** and **8** with $d_{x^2-y^2}$ character found in the HOMO. In [(2,6-$Ph_2C_6H_3$)Cr(THF)], these five occupied orbitals have almost pure d character (see Figure S4 of the Supporting Information), whereas in [(2,6-$Ph_2C_6H_3$)Cr(PMe_3)], HOMO−3 and HOMO−4 exhibit a net overlap of the Cr d_{xz} and d_{yz} orbitals with the p orbitals of the P atom (Figure S5 of the Supporting Information). In a similar fashion, the LUMO and LUMO+1 in [(2,6-$Ph_2C_6H_3$)-Cr(PMe_3)] are hybrid orbitals of π character composed of Cr d_{xz} (LUMO) or Cr d_{yz} (LUMO+1) and p orbitals from both ligand C(ipso) and P centers. In [(2,6-$Ph_2C_6H_3$)Cr-(THF)], LUMO is an empty Cr d_{z^2} orbital with some p_z contribution from C(ipso), but LUMO+1 is a π orbital composed mainly of Cr p_x and p orbitals of one of the phenylic C atoms of the flanking aryl.

A single-point calculation was carried out on the model species [(2,6-$Ph_2C_6H_3$)Cr(η^3:η^6-CH_2Ph)Cr(C_6H_3-2-Ph-1-H)] at the B3LYP/6-31g* level of theory, using the coordinates obtained from the crystal structure of **8**. They show that the six highest occupied orbitals (HOMO to HOMO−5) are mainly 3d in character. Furthermore, the π coordination of the aryl rings to one of the zerovalent Cr atoms as well as the bond between the CH_2 group of the benzyl moiety and the second Cr atom is apparent (see Figure S6 in the Supporting Information).

Discussion

Quintuple-Bonded Dimers 1−4 and Fluoride 5. The synthesis of the series **1**−**4** via reduction of the arylchro-

mium(II) halides ArCrCl (Scheme 1) shows that such compounds can be readily synthesized once an aryl ligand with a suitable steric demand such as Ar′ is employed. In addition, a variety of different X substituents can be introduced into the para position of the central aryl ring with retention of Cr−Cr bonding. However, the reaction of (4-F_3CAr′)CrCl with KC_8 led to the unexpected isolation of the fluoride-bridged dimer **5**. Unfortunately, we were unable to identify the byproducts from this reaction, and the reaction mechanism for the formation of **5** remains unclear. Nevertheless, **5** is noteworthy because divalent chromium fluoride complexes are rare.[43]

The most striking features of the trans-bent solid-state structures (Figure 1) of **1**−**4** are the very short Cr−Cr distances that lie in the narrow range of 1.8077(7) Å in **2** to 1.8351(4) Å in **1** (see Table 2), a variation of only 1.5%. The differences in the Cr−Cr distances do not appear to be correlated with the electron-withdrawing or -donating power of the para substituent. If this were the case, the longest Cr−Cr bond length would be expected for **4**. Rather, it seems likely that the small differences in the Cr−Cr bond lengths of **1**−**4** are due to crystal-packing effects. This notion is supported by the DFT calculations, which show that the effects of para substitution on the geometries of model species (4-XC_6H_4)CrCr(C_6H_4-4-X) (X = H, $SiMe_3$, OMe, and F) are small (Table 3 and Figure S1 of the Supporting Information).

The ^{1}H NMR spectra of **1**−**4** are consistent with the centrosymmetric, trans-bent structures observed in the solid state. The observation of inequivalent C_6H_3-2,6-^{i}Pr$_2$ substituents may be attributed to the persistence of the structure in solution. This is supported by the fact that the *m*- and *p*-H resonances of one C_6H_3-2,6-^{i}Pr$_2$ substituent show an unusal diamagnetic (high-field) shift. These shielded resonances could arise from the ring current generated by the aromatic ring of a C_6H_3-2,6-^{i}Pr$_2$ substituent from the opposite terphenyl ligand or from the effect of magnetic anisotropy of the Cr−Cr quintuple bond (Figure 2). The crystal structures of **1**−**4** show the close proximity of a flanking C_6H_3-2,6-^{i}Pr$_2$ ring from each terphenyl ligand, and the shielded aromatic signals may thus be assigned to the C_6H_3-2,6-^{i}Pr$_2$ substituent that interacts with Cr via weak metal−π interactions. Consistent with their structures, the UV−visible spectra of **1**−**4** show maxima in the narrow range of 482−490 nm, which may tentatively be assigned to $\delta-\delta^*$ transitions. The narrow range of these absorptions also indicates similar bonding properties of **1**−**4** in solution.

Because of the strong Cr−Cr bonding in **1**−**4**, the 10 $3d^5$ valence electrons are fully spin-paired and the compounds exhibit *only* a temperature-independent second-order Zeeman contribution to their molar magnetic susceptibilities; the respective χ'_M values of 0.00112, 0.00082, 0.00150, and 0.00062 emu mol^{-1} of Cr are consistent with the presence of strong Cr^I-Cr^I metal−metal bonding in these essentially diamagnetic compounds. Similar temperature-independent susceptibility has been observed in several multiply bonded transition-metal complexes.[43−48] There appears to be no correlation between the χ'_M values and the Cr−Cr bond distances. Furthermore, there is no obvious reason why χ'_M is the highest for **3**. The measurement of very small magnetic susceptibilities can be very sensitive to errors in the sample mass. However, an error of ±10% in the sample mass will change the χ'_M values reported above by at most ±0.00002 emu mol^{-1} of Cr, and thus such a mass error cannot account for the observed differences. The presence of trace impurities in the range of ca. 0.5−3% is not surprising given the high air and moisture sensitivity of these compounds. While we have modeled these contributions to the magnetic susceptibility assuming that they originate from high-spin Cr^{II} centers, small traces of Cr^{III} impurities could also be used to model the behavior.

The Cr−Cr bonding in **1** has already been discussed in detail elsewhere.[16,49] It was concluded that this compound features a strong metal−metal bond[50] with a formal bond order of 5.[51] This view is now supported by the experimental fact that the Cr−Cr formal quintuple bond in these compounds is not very susceptible to electronic charge induced by the para substituents at the central aryl ring. The results of the DFT calculations reproduce the same bonding situation in all four Cr−Cr dimers (**1**−**4**) and indicate the presence of a strong multiple bond that is rather insensitive to changes at the central aryl ring (Table 3 and Figure S1 of the Supporting Information). This may be contrasted with the behavior of the compounds Ar′SnSnAr′[20a] and Me_3Si-4-Ar′SnSnAr′-4-$SiMe_3$,[20b] where dramatically different degrees of trans bending of the structures is observed.

The strong trans bending in the ArCrCrAr species appears to be mainly a result of s−d hybridzation and was predicted from computations for related H- and Me-substituted model species.[52,53] It is tempting to take the view that the apparent secondary interaction with the flanking aryl ring is a result of the tendency of the Cr to attain an 18-electron configuration (i.e., Cr = 6 electrons, σ-Ar = 1 electron, and π-Ar′ = 6 electrons and 5 electrons from a neighboring Cr to afford a total of 18 valence electrons). However, this does not appear to be the case, and the calculations indicate that the Cr flanking ring interaction is relatively weak. The interaction

(43) (a) Solans, X.; Font-Altaba, M.; Brianso, J. L.; Soalns, A. *Cryst. Struct. Commun.* **1982**, *11*, 1199. (b) Clerac, R.; Cotton, F. A.; Daniels, L. M.; Dunbar, K. R.; Murillo, C. A. *Inorg. Chem.* **2000**, *39*, 752. (c) Berry, J. F.; Cotton, F. A.; Fewox, C. S.; Lu, T. *Dalton Trans.* **2004**, 2297.

(44) Cotton, F. A.; Daniels, L. M.; Lei, P.; Murillo, C. A.; Wang, X. *Inorg. Chem.* **2001**, *40*, 2778.

(45) Ford, P. D.; Larkworthy, L. F.; Povey, D. C.; Roberts, A. J. *Polyhedron* **1983**, *2*, 1317.

(46) Bilgrien, C. J.; Drago, R. S.; O'Connor, C. J.; Wong, N. *Inorg. Chem.* **1988**, *27*, 1410.

(47) Cotton, F. A.; Chen, H.; Daniels, L. M.; Feng, X. *J. Am. Chem. Soc.* **1992**, *114*, 8980.

(48) Clérac, R.; Cotton, F. A.; Daniels, L. M.; Donahue, J. P.; Murillo, C. A.; Timmons, D. J. *Inorg. Chem.* **2000**, *39*, 2581.

(49) Landis, C. R.; Weinhold, F. *J. Am. Chem. Soc.* **2006**, *128*, 7335.

(50) The Cr−Cr bond energy has been estimated to be 76 kcal mol^{-1} in the model compounds PhCrCrPh.[27]

(51) The *formal* bond order is assigned on the basis that five singly occupied orbitals from each Cr participate in the bonding. However, the *effective* bond order is smaller than 5 because of the interaction of metal−metal bonding and antibonding orbitals and has been calculated to be 3.52 for the model complex PhCrCrPh at the CASSPT2 level of theory.

may have a small weakening effect on the Cr−Cr bond through competition for the Cr d orbitals that are otherwise involved in metal−metal bonding. It could also be argued that the π interaction could induce an "artificial" shortening of the Cr−Cr distance by the enforcement of a short "bite" distance. However, calculations on the realistic model species Ar′CrCrAr′ and Ar*CrCrAr* afford Cr−Cr distances similar to those experimentally observed, and such a proposal is unnecessary to account for the short Cr−Cr distances (Table 4). The secondary interaction is best described as an $\eta^1-\eta^3$ coordination, which is much weaker than the σ bond between Cr and C(ipso) of the central aryl ring (Table 2).[54]

The solid-state structure of **5** resembles that of other halide-bridged chromium(II) dimers such as $[Ar'Cr(\mu\text{-}Cl)]_2$,[26] with the difference that there is also a coordinating THF ligand and no secondary Cr−C interaction to one of the flanking C_6H_3-2,6-^{i}Pr$_2$ substituents.[54] The Cr−F distances are slightly longer than those in the chromium(III) complex $[Cp^*_4Cr_4F_5Cl_2]PF_6$,[55] which appears to be the only other structurally authenticated, organometallic chromium fluoride. The square-planar coordination geometry is expected for four-coordinate Cr^{II} centers, and the Cr^{II}−Cr^{II} distance of 3.109(2) Å indicates that metal−metal interactions are weak.

The magnetic properties of **5** are fully consistent with its dimeric structure. The small exchange-coupling constant of -2.5 cm^{-1} is typical of dimeric complexes in which two bridging ligands subtend angles of ca. 90°;[26] in **5**, the two bridging Cr−F−Cr angles are 102.11(7)°. The absence of a Cr−Cr bond was further supported by the Kohn−Sham orbitals of the model compound $[(2,6\text{-}Ph_2\text{-}4\text{-}F_3CC_6H_2)Cr(\mu\text{-}F)(THF)]_2$, which revealed no apparent bonding between the two Cr centers and is thus in agreement with the structural and magnetic data. The weak, extremely broad absorption at 538 nm observed in the UV−visible spectrum is characteristic of halide-bridged dimers such as $[Ar'Cr(\mu\text{-}Cl)]_2$[26] and may be assigned to a d−d transition.

Monomers 6 and 7. The observation that substitution on the central aryl ring had relatively minor effects on the structures of ArCrCrAr complexes prompted us to investigate the effects of variation of the substitution on the flanking aryl rings. This was despite the fact that geometry optimizations of the dimers ArCrCrAr, carrying the increasingly crowded ligand sequence Ar = C_6H_3-2,6-Ph$_2$, Ar′, and Ar*, indicated that changes in the flanking aryl rings of the terphenyl ligands had relatively little effect on the Cr−Cr quintuple bonding (Table 4 and Figure S2 of the Supporting Information). The largest difference involving a lengthening of the Cr−Cr bond is observed when the size of the ligand is increased from Ph to C_6H_3-2,6-Ph$_2$. Further substitution on the flanking aryl rings resulted only in the increased distortion of the angles at the C(ipso) atom between C_6H_3-2,6-Ph$_2$ and Ar*. The difference between the two C(ortho)−C(ipso)−Cr angles[56] is 21.9° for the more crowded Ar*CrCrAr* species [C1−C(ipso)−Cr = 111.9°; C2−C(ipso)−Cr = 133.8°], whereas the analogous difference in Ar′CrCrAr′ is about 17°.[23,57] The presence of the additional ^{i}Pr groups in the para positions of the flanking rings causes increased bending of the flanking aryls away from the CrCr core in the Ar*CrCrAr* molecule. The steric repulsion between the two Ar* ligands is also evident in close contacts between two flanking 2,4,6-^{i}Pr$_3$C$_6$H$_2$ substituents from the Ar* ligands, which are much shorter than the sum of the van der Waals radii of the interacting atoms.[58]

To assess the effect of such steric congestion experimentally, our initial attention was inevitably focused on the C_6H_3-2,6-(C_6H_2-2,4,6-^{i}Pr$_3$)$_2$ (Ar*) ligand. Unfortunately, the attempted synthesis of Ar*CrCrAr* by reduction of Ar*CrCl with KC_8 did not lead to characterizable products. Consequently, we turned to the related ligand C_6H_1-2,6-(C_6H_2-2,4,6-^{i}Pr$_3$)$_2$-3,5-^{i}Pr$_2$, abbreviated 3,5-^{i}Pr$_2$Ar*, whose synthesis we reported recently.[28] In this ligand, the flanking rings remain unchanged from those in Ar* but the central ring now carries ^{i}Pr groups at the meta positions. This substitution introduces rigidity into the structure and improves the crystallization tendency of its derivatives by hindering rotation of the flanking C_6H_2-2,4,6-^{i}Pr$_3$ (Trip) substituents and may further increase the steric protection afforded the reactive metal center to which it is attached. Accordingly, it was expected that the use of this ligand at Cr would yield the dimer 3,5-^{i}Pr$_2$Ar*CrCrAr*-3,5-^{i}Pr$_2$ with a distorted core geometry similar to that expected for Ar*CrCrAr*. To our surprise, when (3,5-^{i}Pr$_2$Ar*)CrCl was reduced with KC_8, the monomer **6** was obtained in moderate yield after removal of the solvent and extraction with hexanes. In effect, the formation of the Cr−Cr bond is prevented by the steric pressure of the ligand. Analogously, **7** was isolated when the reaction was carried out in the presence of an excess of PMe$_3$. Compounds **6** and **7** are not only the first examples of two-coordinate chromium(I) complexes,[59,60] they are also the first two-coordinate open-shell transition-metal complexes in the 1+ oxidation state.[60] Both **6** and **7** have nearly linear coordination geometries (Figure 7 and Table 5). The Cr−C(ipso) (Table 5) bond lengths 2.087(8) and 2.116(2) Å are only slightly shorter than those observed in the dimeric compounds **1**−**4** (Table 2) but longer than those observed in the quasi-four-coordinate arylchromium(II) chloride complex $[Ar'CrCl]_2$ [Cr−C(ipso) = 2.037(2) Å].[26] The Cr−O

(52) Weinhold, F.; Landis, C. R. *Chem. Educ.: Res. Pract. Eur.* **2001**, *2*, 91.

(53) Weinhold, F.; Landis, C. R. *Valency and Bonding*; Cambridge University Press: Cambridge, U.K., 2005; pp 555−559.

(54) A secondary η^1 interaction between Cr and a flanking aryl ring is observed in the chromium(II) halide $[Ar'Cr(\mu\text{-}Cl)]_2$.[26]

(55) Thomas, B. J.; Mitchell, J. F.; Theopold, K. H.; Leary, J. A. *J. Organomet. Chem.* **1988**, *348*, 333.

(56) Note that the C(ortho)−C(ipso)−Cr angles are very similar, but not identical, in the optimized PhCrCrPh model; such an effect could be associated with an agostic Cr−H interaction.

(57) Compare the respective values in the crystal structure of **1**: C2−C1−Cr1 = 114.34(7)°; C2−C1−Cr1 = 131.74(7)°.

(58) Interligand C−H distances for the methine proton of the *p*-^{i}Pr group are 2.559−2.797 Å, while the sum of the van der Waals radii of C and H is 3.1 Å. Compare: Wibert, N. *Holleman−Wiberg: Lehrbuch der Anorganischen Chemie*, 101st ed.; Walter de Gruyter: Berlin, 1995.

(59) For examples of two-coordinate chromium(II) complexes, see the following. (a) [Cr(NMes{BMes$_2$})$_2$]: Bartlett, R. A.; Chen, H.; Power, P. P. *Angew. Chem., Int. Ed.* **1989**, *28*, 316. (b) [Cr(NPh{BMes$_2$})$_2$]: Chen, H.; Bartlett, R. A.; Olmstead, M. M.; Power, P. P.; Shoner, S. C. *J. Am. Chem. Soc.* **1990**, *112*, 1084. (c) [Cr(SAr*)$_2$]: Nguyen, T.; Panda, A.; Olmstead, M. M.; Richards, A. F.; Stender, M.; Brynda, M.; Power, P. P. *J. Am. Chem. Soc.* **2005**, *127*, 8545.

bond length in **6** [Cr1−O1 2.062(5) Å] and the Cr−P bond distance in **7** [2.4646(5) Å] are unexceptional.[61,62] No secondary interaction between chromium and the flanking aryl rings of the (3,5-^{i}Pr$_2$−Ar*) ligands could be observed. It is noteworthy that neither **6** nor **7** contain π-acid ligands such as CO which are normally required in low oxidation state organometallic species to oppose charge build-up at the metal in accordance with the Pauling's electroneutrality principle.[63] Because of the low number of ligands in **6** and **7** there is no excessive charge buildup and accordingly no requirement for π-acceptor ligands.

The magnetic susceptibilities of **6** and **7** (Figure 9) are consistent with high-spin Cr^{I} with a 3d^5 electronic configuration and a nominal ^{6}A$_1$ ground state in a highly distorted coordination environment, a configuration that would have a virtually temperature-independent effective magnetic moment, μ_{eff}, of 5.92 μ_B. The agreement with the expected moment is excellent for **6**, but the 6.17 μ_B moment observed for **7** is somewhat high probably because of the loss of some of the cocrystallized hexane during the preparation of **7** for magnetic studies. If it is assumed that 80% of the hexane is lost during this process, a value of 5.92 μ_B is obtained. The very small deviation of $1/\chi'_M$ of **6** and **7** from the expected linear behavior below 10 and 7 K, respectively, is probably the result of a very small zero-field splitting of the Cr^{I} ground state by its highly distorted environment or a trace of an unknown impurity. The lower than expected susceptibility below ca. 10 K is due to either a small zero-field splitting or some weak Cr^{I}−Cr^{I} antiferromagnetic exchange coupling, or perhaps a combination of both.

Analysis of the ^{1}H NMR spectra of **6** and **7** was complicated by their paramagnetism, which leads to dramatically broadened signals, and by their instability in a C_6D_6 solution. It appears that in both cases aromatic solvent molecules replace the THF and PMe$_3$ ligands initially, but the resulting chromium(I) arene complexes are apparently unstable and decompose. This is indicated by the observation of a complex product mixture in their ^{1}H NMR spectra and by the isolation of **8** when toluene is the solvent (vide infra).

The UV−visible spectra of both compounds (in hexanes) showed quite similar transitions at 430 nm (**6**) and 442 nm (**7**). Presumably, these are associated with transitions from half-occupied d orbitals to the LUMO orbital, which is an empty Cr d_{z^2} orbital with some contribution from the p_z orbital of ligand C(ipso) for **6** but with a much greater p-orbital contribution in the phosphine-complexed **7**, according to spin-unrestricted DFT calculations on model complexes.

As reported previously, calculations on the model complexes [(2,6-Ph$_2$C$_6$H$_3$)Cr(THF)] and [(2,6-Ph$_2$C$_6$H$_3$)Cr(PMe)$_3$] each yielded a sextet ground state,[29] which is in agreement with what is experimentally observed. The five highest molecular orbitals (which are singly occupied) are mainly of d character. Subtle differences are observed between the compounds in the ordering of the d orbitals as a result of mixing with the ligand orbitals. It remains to be seen to what extent these affect the reactivities of these compounds. Because of the difficulty in the treatment of the excited states in the open-shell d^5 model molecules, attempts to calculate the electronic transitions for the monomeric species in order to understand the experimental UV−vis spectra have so far been unsuccessful. Further theoretical work is in progress to elucidate the electronic structures of **6** and **7**.

Chromium(0)/Chromium(II) Sandwich Complex 8. Two recent publications have demonstrated the high in situ reactivity of low-coordinate chromium(I) species supported by the nacnac ligand (nacnac = {N(C$_6$H$_3$-2,6-^{i}Pr$_2$)CMe}$_2$-CH), which is sterically related to the terphenyl ligands employed in our studies. Reduction of the chromium(II) halide precursor [Cr(μ-I)(nacnac)]$_2$ in dinitrogen in THF led to a dinuclear dinitrogen complex [{Cr(nacnac)}$_2$(μ-N$_2$)],[64] while the "inverted sandwich" [{Cr(nacnac)}$_2$(η^6:η^6-PhCH$_3$)],[65] in which a toluene molecule has been inserted between two Cr^{I} centers, was obtained from the reduction of the analogous chromium(II) chloride complex in toluene. The ability of the latter complex to exchange different arene ligands with retention of its inverted sandwich structure is particularly noteworthy. In contrast to this behavior, an immediate color change was observed when toluene was added to the crude product obtained from the reaction of (3,5-^{i}Pr$_2$Ar*)CrCl with KC$_8$ at room temperature, and the mixed-valent dinuclear complex **8** was isolated in 44% yield. Although the structural arrangement of **8** (Figure 8) is related to that of [{Cr(nacnac)}$_2$(η^6:η^6-PhCH$_3$)], a striking difference is that in **8** a methyl C−H bond of toluene has been cleaved while an Ar*-3,5-^{i}Pr$_2$ ligand is protonated to give Ar*-1-H-3,5-^{i}Pr$_2$. The structure of **8** contains an anionic CH$_2$Ph$^-$ ligand at its center whose coordination resembles that in the chromium(I)/chromium(III) complex [Cp*Cr(η^1-CH$_2$Ph)(η^3:η^6-CH$_2$Ph)CrCp*] (Cp* = C$_5$Me$_5$), which was formed by thermal rearrangement of [Cp*Cr(μ-CH$_2$Ph)]$_2$.[55] However, in **8**, Cr1 is bound to two anionic ligands (3,5-^{i}Pr$_2$Ar*$^-$ and CH$_2$Ph$^-$) and thus has a 2+ oxidation state. The coordination environment of the second chromium, Cr2, closely resembles the sandwich structure of (bis)benzenechromium and related compounds,[66] and this chromium has a zero oxidation state. The reaction may thus be regarded as a disproportionation of a presumably unstable chromium(I) intermediate 3,5-^{i}Pr$_2$-Ar*Cr·PhMe. The observation of a deprotonated CH$_2$ group in the benzyl anion is supported by the relatively short C−C distance [C1−C7 = 1.459(4) Å] and by the observation of two H atoms bound to C7 in the X-ray structure. The strong interaction between Cr1 and the benzylic C atom, C7, is reflected in the bending of C7 out of the plane of the phenyl

(60) Power, P. P. *Comments Inorg. Chem.* **1989**, *8*, 177. Power, P. P. *Chemtracts: Inorg. Chem.* **1994**, *6*, 181.
(61) The Cr−O distances of 88 Cr−THF complexes in the Cambridge Crystal Structure Database (version 5.27, Aug 2006) range from 1.994 to 2.449 Å, with a median of 2.097 Å.
(62) The Cr−P distances of 53 Cr−PMe$_3$ complexes in the Cambridge Crystal Structure Database (version 5.27, Aug 2006) range from 2.288 to 2.525 Å, with a median of 2.383 Å.
(63) Pauling L. *The Nature of the Chemical Bond*, 3rd ed.; Cornell University Press: Ithaca, NY, 1960; p 172f.
(64) Monillas, W. H.; Yap, G. P. A.; MacAdams, L. A.; Theopold, K. H. *J. Am. Chem. Soc.* **2007**, *129*, 8090.

ring (C7−C1−centroid = 169.3°). The benzyl ligand is bound in an allylic fashion, with bonding parameters similar to [Cp*Cr(η^1-CH_2Ph)(η^3:η^6-CH_2Ph)CrCp*][55] and [Cp*Cr(C_6F_5)(η^3-CH_2Ph)],[67] which appear to be the only other structurally characterized complexes of Cr with an η^3-coordinated benzyl ligand. The secondary Cr−C113 interaction seen for the anionic (3,5-^{i}Pr$_2$Ar*)$^-$ ligand is reminiscent of the motif found in the Cr^I−Cr^I metal−metal-bonded dimers **1**−**4** (Figure 1 and Table 2), although it is weaker in **8**. The protonation of the second terphenyl ligand is confirmed by the observation of a H bound to the C(ipso) of its central aryl ring [C201−H201 = 0.93(3) Å].[68]

The magnetic properties of **8** (Figure 9), obtained in an applied field of 0.01 T, are consistent with the presence of one Cr^{II} center, as is indicated by the structural and spectroscopic results. If one assumes that Cr2 is Cr^0, its six valence electrons are fully spin-paired and thus Cr2 will make no paramagnetic contribution to the magnetic susceptibility of **8**. In contrast, Cr1 is predicted to have a $3d^4$ electronic configuration and should exhibit a spin-only μ_{eff} of 4.90 μ_B in the absence of any long-range magnetic interactions between the Cr1 sites; these interactions should be small because of the long 9.724 Å Cr1−Cr3 intermolecular distance.

In view of the related, stable nacnac complex [{Cr(nacnac)}$_2$(μ-η^6:η^6-$PhCH_3$)],[65] the first step in the formation of **8** very likely involves the interaction of **6**, present in the reaction mixture, with toluene. Coordinative unsaturation at a Cr center may then induce the migration of a methyl proton from toluene to one of the 3,5-^{i}Pr$_2$Ar* ligands. However, other possible mechanisms cannot be excluded because of the difficulty in isolating the labile intermediates in this reaction. Nevertheless, the formation of **8** highlights the unusual reactivity of low-coordinate, univalent chromium species such as **6** and **7** and makes them very attractive subjects for future reactivity studies.

Conclusions

The results show that the reduction of divalent ArCrCl precursors is a general route to ArCrCrAr compounds, although the choice of substituent X in the ligands Ar′-4-X is limited by substituent reactivity, as indicated by the isolation of **5** from the reaction of (4-F_3CAr′)CrCl with KC_8. Analysis of the structures, spectroscopic properties, and magnetic behavior of the dimers **1**−**4** revealed only small effects by the substituent at the para position of the central aryl ring on the Cr−Cr bond. The introduction of the very bulky 3,5-^{i}Pr$_2$Ar* ligand, which features additional ^{i}Pr substituents on the flanking aryl rings of the terphenyl ligands, has a dramatic effect on the structure of the resulting products. The formation of a dimer (3,5-^{i}Pr$_2$Ar*)CrCr(3,5-^{i}Pr$_2$Ar*) is prevented by its steric properties, and monomeric complexes **6** and **7** were isolated. Compounds **6** and **7** are the first stable two-coordinate chromium(I) compounds, whereas the only previously known examples involved chromium(II) and rare examples of open-shell σ-bonded transition-metal complexes with an oxidation state of less than 2+. The isolation of **8** after the addition of toluene to the crude reaction product of **6** underlines the fact that different substitution patterns in the terphenyl ligands not only have structural significance but also influence reactivity. The remarkably facile activation of a C−H bond of toluene bodes well for a systematic reactivity study of the coordinatively unsaturated chromium(I) compounds **6** and **7**, which is currently underway.

Acknowledgment. We are grateful to Dr. Andreas Ehlers and Prof. Koop Lammertsma (Vrije Universiteit Amsterdam) for access to computing facilities at the VU and valuable advice. Peter Klavins (magnetic measurements) and Marilyn M. Olmstead (X-ray crystallography) are thanked for assistance. Financial support from the National Science Foundation, the Alexander von Humboldt Foundation (Feodor-Lynen-Fellowship for R.W.), and the Max Kade Foundation (fellowship for R.C.F.) is gratefully acknowledged.

Note Added after ASAP Publication. This article was published ASAP on November 29, 2007, with incorrect reference sequencing. The correct version was published on December 3, 2007.

Supporting Information Available: Synthesis and characterization of 4-XAr′I and Li(4-XAr′) (X = F and CF_3), details of theoretical investigations, pictures of frontier orbitals, crystallographic data in CIF format, and complete refs 31, 38, and 40c. This material is available free of charge via the Internet at http://pubs.acs.org.

Note Added in Proof. After this paper had been submitted, the synthesis and structure of a chromium dimer which had a very short Cr−Cr bond (1.8028(9) Å) with quintuple character was reported. See: Kreisel, K. A.; Yap, G. P. A.; Dimitrenko, O.; Landis, C. R.; Theopold, K. H. *J. Am. Chem. Soc.* **2007**, *129*, 14162.

IC702112E

(65) Tsai, Y.-C.; Wang, P.-Y.; Chen, S.-A. *J. Am. Chem. Soc.* **2007**, *129*, 8066.
(66) Weiss, E.; Fischer, E. O. *Z. Anorg. Allg. Chem.* **1956**, *10b*, 665. Keulen, E.; Jellinek, F. *J. Organomet. Chem.* **1966**, *5*, 490.
(67) Mani, G.; Gabbaï, F. P. *Angew. Chem., Int. Ed.* **2004**, *43*, 2263.
(68) The H atoms of the benzylic segment and the C(ipso) atom of the Ar*-1-H-3,5-^{i}Pr$_2$ ligand were located on the Fourier difference map and refined freely for both crystallographically independent molecules in the X-ray crystal structure of **8**.